Master's thesis

NTNU
Norwegian University of Science and Technology
Faculty of Information Technology and Electrical Engineering
Department of Electric Power Engineering

Magnus Bøe

Future Design of Subsea High Voltage Cables for Offshore Renewables - Effect of Static Mechanical Stresses on the Insulation Lifetime

Master's thesis in Electric Power Engineering
Supervisor: Frank Mauseth
Co-supervisor: Karl Magnus Bengtsson
June 2022

NTNU
Kunnskap for en bedre verden

Magnus Bøe

Future Design of Subsea High Voltage Cables for Offshore Renewables - Effect of Static Mechanical Stresses on the Insulation Lifetime

Master's thesis in Electric Power Engineering
Supervisor: Frank Mauseth
Co-supervisor: Karl Magnus Bengtsson
June 2022

Norwegian University of Science and Technology
Faculty of Information Technology and Electrical Engineering
Department of Electric Power Engineering

NTNU

Kunnskap for en bedre verden

Preface

This master's thesis is written at the Norwegian University of Science and Technology in the spring of 2022 and is included as a final part of the master's program Electric power engineering. The title of this thesis is: Future Design of Subsea High Voltage Cables for Offshore Renewables - Effect of mechanical stresses on the insulation lifetime.

This thesis is a continuation of the project assignment from the autumn of 2021. The problem description of this thesis is as follows: High voltage subsea cables are essential e.g. to facilitate renewable offshore energy installations such as wind and solar farms. Today, polymeric AC subsea cables rated up to 36 kV are generally of a "wet design" type, while for higher voltages, "dry designs" are applied where the cable is equipped with an enclosing metallic water barrier. Lately, there has been a great interest in increasing the voltage rating of wet designed cables to be used for i.e. inter-array connections in offshore wind farms and floating installations. The main advantage of a "wet design" at higher voltage levels is cost savings as the metallic water barrier is eliminated. Wet designed high voltage cables are also a very attractive solution for dynamic cables, where the metallic water barrier of a dry design cable can be an issue due to mechanical fatigue. In addition to the dynamic mechanical stresses, cables can simultaneously be subjected to static mechanical stresses, e.g. stresses from 3 core lay-up and exit J-tube, where the side facing the center will be compressed while the other side will be stretched. The static mechanical stresses can be significant. Thus, it is important to investigate how the static mechanical stress with the combined effect of the electric field, humidity, and temperature influences the lifetime of XLPE cable insulation. The proposed project will be mainly experimental. The results will be an important input to the design criteria of the next generation of wet designed power cables for offshore renewables.

I want to give a special thanks to my supervisor at NTNU, Frank Mauseth, for excellent guidance and feedback. I would like to thank Amar Abideen for supporting me through this project and being an exceptional discussion partner. Also, I would like to thank Sverre Hvidsten and Halvard Faremo at Sintef for providing superb answers to my questions and providing with information that is not accessible through research articles, but comes from years and years with experience in the field.

Summary

Today, a wet-design cable is normally rated for up to 36 kV. Recently there has been a great deal of interest in increasing the voltage so they can be used for inter-array connections in offshore wind farms where they are exposed to both dynamic and static mechanical stresses. However, wet-design cables are subjected to a degradation mechanism called water treeing. Water treeing can occur in polymer-insulated cables where water and an electric field are present. Water trees reduce breakdown voltage strength and reduces the lifetime of the cables. The aim for this report was to investigate how static mechanical stresses affect this newly developed wet-design cable, with focus on the length of the water trees observed in the cables.

An aging rig was set up and confirmed functional in the autumn of 2022. Ten samples of 12 kV wet-design cables were aged with static mechanical stress. The mechanical stress were induced by bending the cables around three different pipes with different diameters, which gives a stretch of 4%, 6% and 12%, simultaneous the same amount in compression force was applied. These cables were then connected to the aging rig. The rig consist of a large water bed that were heated to 40 °C. All cables were connected in parallel to a bus bar and energized with 30 kV 50 Hz AC. The cables were then aged in a total of six months, where the first cable was disconnected and inspected after one month, with the other cables following the same procedure with one month intervals.

After the aging period the insulation of the cable was cut into helicoids, and dyed. During the microscope analysis the longest bow-tie tree in stretch and compression zone was recorded, as well as length of vented trees if observed in the different zones. In addition, the two longest vented trees were examined in more detail to investigate the cause of initiation. This procedure was used for the three different mechanical stresses.

The results documented indicate the average maximum length of the bow-tie trees are longer in the zone applied with stretch compared to the compression zone. It was also documented that 8% increase in stretch, gives 7% increase in length of the bow-ties. Whereas the same increase in compression force yields a 10% increase in length of the bow-ties.

The results show no difference between stretch and compression zone in the amount of vented water tree observed. The longest tree observed was a vented tree of 250 µm, initiated from the inner semi-conductor, which is 7% of the total thickness. The low number of vented trees in addition to the short lengths can indicate a good design that is very resistant to water tree growth.

Sammendrag

I dag er normalt en våtdesign kabel klassifisert for opptil 36 kV. I det siste har det vært en stor interesse for å øke spenningen slik at de kan brukes til inter-array forbindelser i vindparker til havs hvor de utsettes for både dynamisk og statisk mekanisk krefter. Kabler med våtdesign kan imidlertid være utsatt for en nedbrytningsmekanisme kalt vanntre. Dannelse av vanntre kan forekomme i polymerisolerte kabler der vann og et elektrisk felt er tilstede. Vanntrær reduserer gjennomslagsspenning og reduserer levetiden til kablene. Målet med denne rapporten var å undersøke hvordan statisk mekaniske påkjenninger påvirker den nyutviklede våtdesign kabelen, med fokus på lengden på vanntrærne observert i kablene.

En aldringsrigg ble satt opp og bekreftet fungerende høsten 2022. Ti prøver av 12 kV kabler med våtdesign ble aldret med statisk mekanisk påkjenning. Den mekaniske påkjenningen ble indusert ved å bøye kablene rundt tre forskjellige rør med forskjellige diametere, noe som gir en strekk på 4%, 6% og 12%, samtidig ble samme mengde i kompresjonskraft påført. Disse kablene ble deretter koblet til den aldrende riggen. Riggen består av et stort vannbasseng som ble varmet opp til 40 °C. Alle kabler ble koblet i parallell på en samleskinne og spenningssatt med 30 kV 50 Hz AC. Kablene ble deretter aldret i totalt seks måneder, hvor den første kabelen ble koblet fra og inspisert etter en måned, mens de andre kablene følger samme prosedyre med 1 måneds intervaller.

Etter aldringsperioden ble isolasjonen kuttet i helikoider og farget. Under mikroskopanalysen ble det lengste sløyfetreet i strekk og kompresjon sonen registrert, samt lengde på ventilerte trær hvis de var observert i de forskjellige sonene. I tillegg var de to lengste ventilerte trærne undersøkt nærmere for å undersøke årsaken til initiering. Denne prosedyren ble brukt for de tre forskjellige mekaniske påkjenningene.

Resultatene som er dokumentert indikerer gjennomsnittlig maksimal lengde på sløyfetrærne er lengre i sonen som påføres med strekk sammenlignet med kompresjons. Det er også dokumentert at 8% økning i strekk, gir 7% økning i lengde på sløyfertrær. Mens den samme økningen i kompresjonskraft gir en 10% økning i lengden på sløyfene. Resultatene viser at det ikke er noe forskjell mellom strekk og kompresjonssonen når det kommer til mengden av ventilert vanntre observert. Dette gjelder også lengden av de ventilerte trærne. Det lengste treet som ble observert var et ventilert tre på 250 µm som var initiert fra den indre halvlederen. 250 µm i lengde tilsvarer 7% av den totale tykkelsen. Det lave antallet av ventilerte trær i tillegg de korte lengdene kan indikere et godt design som er veldig motstandsdyktig mot vanntrevekst.

Table of Contents

1 Introduction

1.1 Purpose

The purpose of this project is to study water tree growth in a newly developed wet-design XLPE-insulated cables with static mechanical stresses applied. This report includes the setup and procedure of making the test rig of which the cables will be aged, which was done autumn 2021. Further on, the results from the water tree analysis, conclusion and suggestion of further work will be presented.

1.2 Background

The state of art and related work were reviewed, and an identification of the relevant background material were carried out in the project preceding this thesis[1].

There has been increased interest in renewable energy production in the last decade, especially in wind power. Using windmills to harvest energy from wind has been done onshore for over a thousand years. It is not until recently that moving the wind turbines out to sea has been possible.

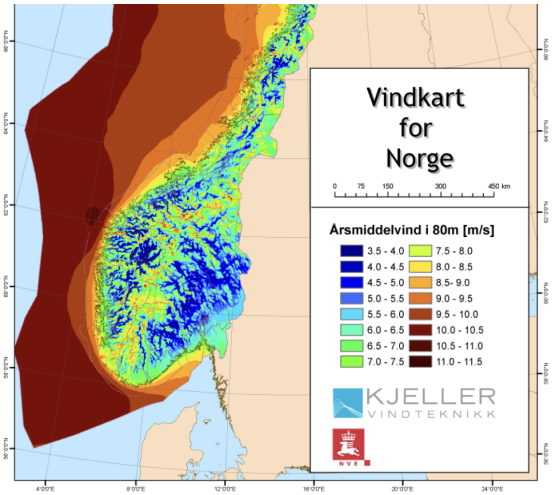

Figure 1: Wind map of Norway[2]

There are some advantages to moving wind farms offshore. This is especially true on the Norwegian continental shelf, where the areas with the highest annual average wind are located offshore, as seen in figure 1. Another benefit is the noise, visual pollution and natural damage are moved to areas where people do not live.

The technology needed to make floating wind turbines in deep-water areas exists. Equinor will turn on the world's largest floating wind farm by the end of 2022, consisting of 11 Siemens Gamesa SG 8.0-167 DD floating wind turbines with a total capacity of 88 MW. The wind turbines are connected to 5 oil rigs and should reduce emissions by 200000 tons of CO_2 and 1000 tons of NO_X every year[3].

There are, however, raised concerns about the long-term costs of these types of

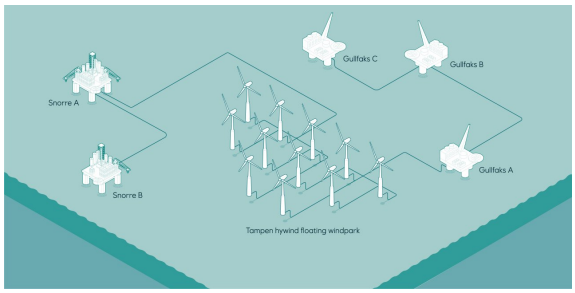

Figure 2: Overview of Hywind Tampen[3]

projects. Not only about the initial investment costs but also the maintenance costs. Floating wind turbines are subjected to large environmental forces, resulting in a dynamic motion that negatively affects dry design cables. The dynamic mechanical stresses will lead to mechanical fatigue in the metallic sheath of the cable, which causes cracks and water ingress pathways. In addition to the dynamic mechanical stresses, cables can also be subjected to static mechanical stresses, for example, from 3 core lay-up and exit J-tube, where the side facing the center will be compressed while the other side will be stretched. Due to these stresses, dry design cables can be ineffective for this application. Therefore there is significant research interest in the development of wet design cables. Not only to make them more resistant against water trees but also to increase the voltage level. The benefits of wet design cables are reducing manufacturing costs, weight reduction, and the ability to withstand more significant mechanical stresses.

It is commonly acknowledged that moisture and electric field together will over time deteriorate XLPE-insulated cables. Where high AC voltage and mechanical stresses accelerate this degradation process even more. At higher voltage levels, water trees grow faster and will eventually cause breakdown leading to complete failure of the cable. Although the first water trees were documented in 1969, there is still much research needed to fully understand the factors leading to the growth and initiation factors of the trees. This knowledge gap makes it difficult for manufacturers to give a reliably estimated cable lifetime.

1.3 Scope

This master thesis is a continuation of the project that started in the autumn of 2021, where the test rig was built to accelerate the aging of XLPE-cables. During this project, ten cables were aged with static mechanical force applied at 4%, 6% and 12% stretch and compression. This was done for six months, where the first cable was inspected after one month, with each cable following in a time step of 30 days. The cables were connected to a busbar in parallel, energized with 30 kV AC at 50 Hz. The temperature was fixed at 40 °C. After the aging period, each cable was cut up into helicoids and analyzed for water trees in the zones where the static mechanical forces was the highest.

1.4 Hypothesis

Previous experiment with triple-extruded cables applied with static mechanical loading indicates that the average maximum length and density of bow-tie and vented trees increases with stretch forces. In the same experiment, the results shows that the exact opposite happens under compression[4]. However, as the cables that are used in this experiment are newer they are most likely to have better resistance to water tree growth. Therefore the mechanical forces can have less impact on the length of the water trees. Nevertheless the same pattern are expected to be found in the cable used in this experiment. It is also expected that increase in stretch (4% - 12%) should influence the results as well as the increase in compression (4% - 12%).

The theory behind this is that the stretch forces plus the Maxwell forces will work in the same direction to increase the formation of crazes as shown in figure 3. The compression forces will thus work in the opposite direction. Reducing the net force acting perpendicular to the craze.

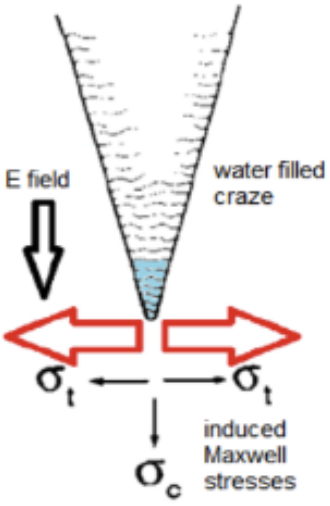

Figure 3: Sketch showing a mechanical model for initiation and growth of vented water trees[5]

It is expected that the average maximum length of the bow-tie and vented water trees will grow in line with increased aging time as documented by T.A. Lindseth [6]. However, as vented water trees should have linear increase in length the bow-ties should have a rapid increase in length in the beginning because of the high moisture available and will almost stop growing after a while as the onset moisture collects within hydrophilic regions. The time needed before the bow-ties reaches is peak growth rate is expected to vary based on the amount of mechanical force applied. As the compression force increases the time before the peak growth rate is reached should also increase.

2 Literature review

The state of art and related work were reviewed, and an identification of the relevant background material were carried out in the project preceding this thesis[1]. Additional information was added to section: 2.2.4 Effect of water treeing on breakdown strength, 2.2.5 The effect of humidity on water tree growth in XLPE-cables and 2.2.6 The effect of mechanical stress on water tree growth in XLPE-cables.

2.1 Manufacturing of XLPE cables

According to Nexans, the production method used to make the cable relevant to this project is state-of-the-art vertical continuous vulcanization. An illustration of this process is shown in figure 4.

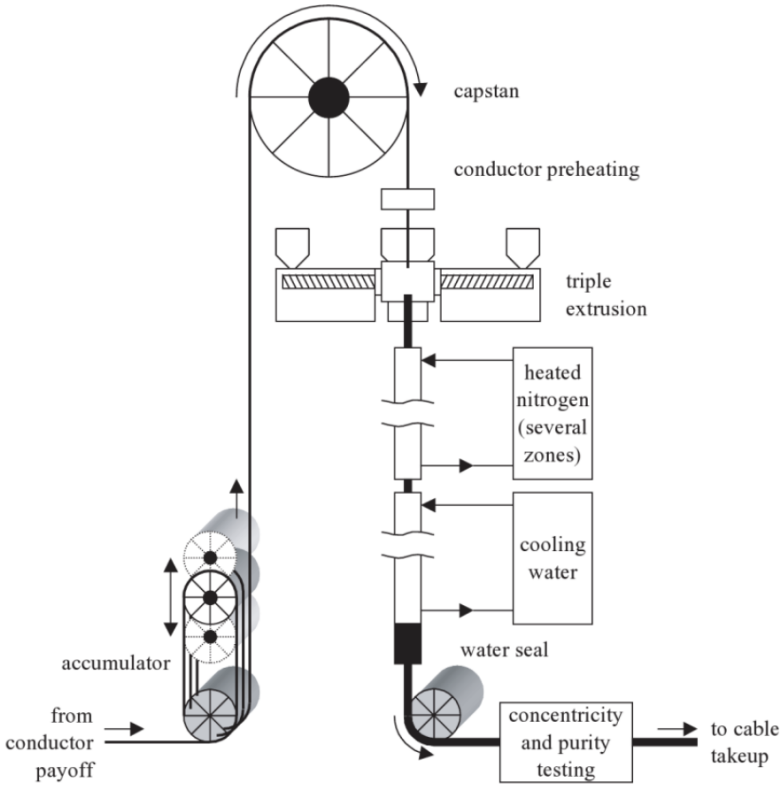

Figure 4: Vertical continuous vulcanization production method[7]

In this production method, the curing tube is arranged vertically. The conductor is inserted from the bottom of the tower, where there are accumulators that allows time for conductors being welded together when the reel runs out and needs to be connected to a new one without stopping the production. The conductor gets pulled to the top of the extrusion tower over the capstan, fed into a preheater, and into a triple extrusion head. After this process, the curing will start, and hot, pressurized nitrogen gas is added. The pressure will ensure that gas-filled voids do not form

from the peroxide decomposition. The vertical alignment of the tube ensures the concentricity of the conductor within the cable core[7].

2.2 Theory

2.2.1 What is a water tree?

Water tree is a degradation mechanism formed in polyethylene and other polymerics when moisture and an electric field is present, which can lead to a decrease in breakdown strength. Previous research shows that several factors play a role in the initiation and growth of water trees, including moisture, electric field, mechanical stress, and impurities[8].

Even though there has been extensive research on this topic, there is not a complete understanding of the initiation mechanism. The predominant theories in regard to the initiation are the mechanical model and electrochemical model[9].

2.2.2 Water tree models

The mechanical model presumes that local mechanical overstressed regions are caused by a mixed reaction of external mechanical stress and Maxwell stresses induced by the electric field[5]. The mechanical forces are presumed to be due to Maxwell stresses that is induced by the strong inhomogeneous field. The AC voltage will act on water molecules present in the cracks or crazes of the insulation. If stresses are sufficiently high, it will lead to crazing zones at the tip. As electric forces attract water into the crazes, the process continues further and further in the insulation[10]. Assuming the water-filled craze is electric conducting, the Maxwell forces acting in the tip of a craze is given by[4]:

$$\sigma = \frac{1}{2}(\epsilon_0 \epsilon_r E^2) \tag{2.1}$$

Where ϵ_0 is the permittivity of vacuum, ϵ_r is the relative permittivity, and E is the electric field. In cases where the field enhancements in crazes are high enough, forces can go as high as 10 MPa, which is sufficiently high enough to create new crazes[4].

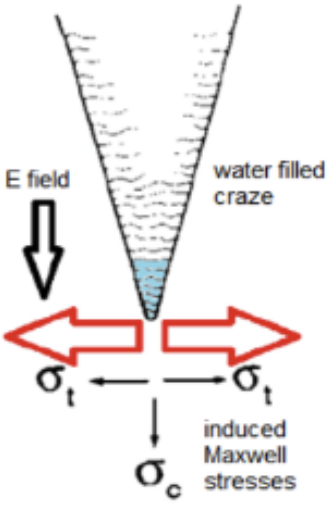

Figure 5: Sketch showing a mechanical model for initiation and growth of vented water trees[5]

The second model that seeks to explain water tree initiation and growth is the electrochemical model. This model explains that the initiation of water trees are a result of localized chemical reactions within the material that is influenced by electric field and water content. Chemical reactions that are affected by electric fields and water content will result in chain splitting and additional hydrophilic areas. The hydrophilic molecules attract water from within the insulation and lead to increased diffusion into condensation points, which again leads to faster chain splitting and water tree growth. These chemical reactions also cause free ions to be dispensed into the water from impurities and forced into cracks by the electric field that form conductive centers. These conductive centers initiate water tree growth as they form the first conductive link to the tip of the crack in the material[11].

2.2.3 Types of water trees

Water trees are observed to have two shapes: Bow-tie trees or vented trees, As illustrated in figure 6.

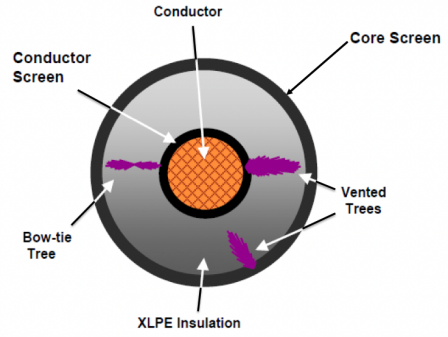

Figure 6: Illustration of water trees[12]

Bow-tie tree initiation point comes from impurities or defects within the insulation. They grow symmetrical outward with the electric field. The growth rate is generally quite steep initially, which rapidly settles down and flattens out, as illustrated in figure 7. This growth pattern happens because of the high moisture available at the beginning and nearly halts as the onset moisture collects within hydrophilic regions. As the growth of bow-ties saturates, it is unlikely a source of a breakdown in the cable, but the bow-tie can have significant influence on reducing the breakdown strength of the cables. Bow-tie can also develop into a vented tree if it initiates close to the insulation screen[11].

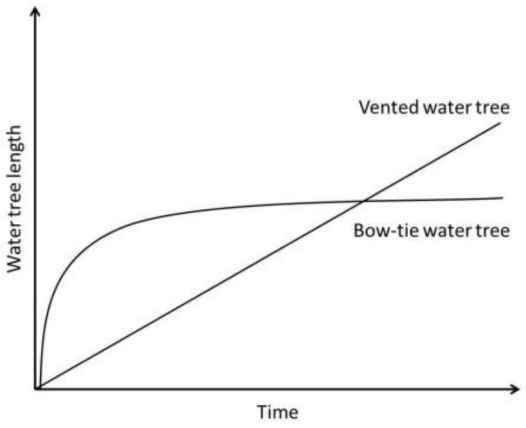

Figure 7: Growth rates of vented water trees and bow-ties[11]

Another type of water trees is the vented water trees, which initiate from inner or outer screen, then grows to fully penetrate the insulation. The source or initiation point often comes from unevenness, abnormalities like trapped hydrophilic particles, or damage on the semiconducting screen. As the vented tree has supplementing water source at the root, the water tree has a steady growth compared to bow-tie water trees[8].

2.2.4 Effect of water treeing on breakdown strength

Previous research has proven that water trees reduce the breakdown strength of XlPE-cables [13]. This kind of degradation can be caused by both vented water tree and bow-ties. The reduction in breakdown strength caused by a vented water tree is determined by the length of the tree in respect to insulation thickness, as illustrated in figure 8. A single Bow-tie tree usually do not reduce the breakdown strength of the insulation due to the limited growth of the tree. However in areas where the density of bow-ties are high the degradation can be reduced. In these cases the factor is governed by the cluster's average tree length and density of bow-ties[14].

Within treed regions the electric field is enhanced drastically. The increased electric field also increases the possibility of partial discharges from these regions. There has been recorded partial discharges from voids as small as $\leq$ 5µm [13][14]. The partial discharges from these small voids can lead to breakdowns at much lower field

strengths than the cable is designed to withstand. In addition, this also increases the probability of failure earlier then expected[13][14].

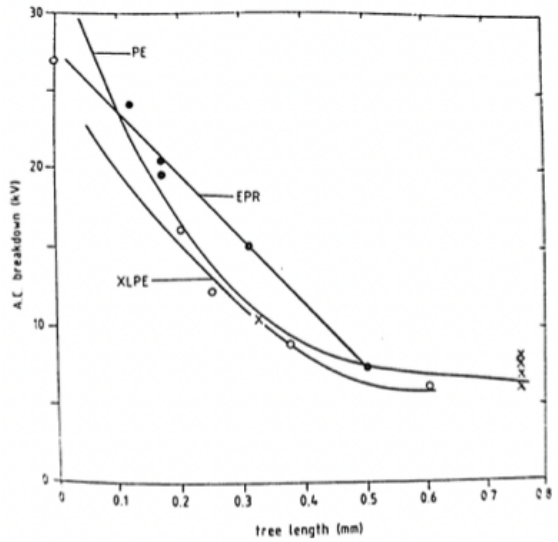

Figure 8: Breakdown strength as a function of water tree length[13][14]

2.2.5 The effect of humidity on water tree growth in XLPE-cables

In contrary to glass and metals, water can move through polymers. By using Henry's law together with Fick's law, water ingress can be characterized. Henry's law defines that water concentration $\rho_{(w,s)}$ is proportional to water vapor pressure above the surface $p_{(w,s)}$ times the solubility coefficient for water within the polymer[15]:

$$\rho_{(w,s)} = S \cdot p_{w,s} \tag{2.2}$$

where $\rho_{(w,s)}$ is the water concentration at polymer surface. S is the solubility coefficient for water within the polymer, and $p_{w,s}$ is the water vapor pressure above the surface.

Ficks law defines that the flow rate per unit area is proportional to diffusion coefficient times species concentration gradient[15]:

$$j = -D \cdot \nabla\rho \tag{2.3}$$

where j is the flow rate per unit area. D is the diffusion coefficient and $\nabla\rho$ is the species concentration gradient.

The diffusion coefficient is dependent on temperature and can be expressed as:

$$D = D_0 \cdot exp(\frac{-E_d}{RT}) \tag{2.4}$$

where D_0 is the material constant. E_d is the activation energy for diffusion reaction. R is the universal gas constant and T is the absolute temperature.

The growth rate of water trees is heavily affected by the availability of water in the surrounding insulation. Three phases of water tree growth can be identified where water diffuses into the insulation:

1. Phase 1: $RH < 70\%$ - Only diffusion, no water tree growth.
2. Phase 2: $70\% < RH < 100\%$ - Tree growth at a reduced rate.
3. Phase 3: $100\%\, RH$ - Water tree growth at full rate.

In the first phase, the relative humidity is too low for water trees to initiate. This phase is what is usually considered relevant to the lifetime of a cable. In the second phase, the humidity is sufficient for initiation and growth of water trees. However, a relative humidity lower than 100% limits the growth rate, as water trees need water in liquid form to grow. The condensation of water at water soluble particles such as salts will be important in this phase. In the third phase, the insulation is saturated with water. High availability of water will support water tree initiation and growth. In figure 9, the different phases are illustrated for water diffusion into the insulation of an XLPE insulated cable. The time duration of the second phase is much longer than the first phase. This means that in a cable where the relative humidity is high enough that water trees have started to grow, the growth rate will be limited for a long time. It is therefore important to consider also the time from 70% to 100 % RH when discussing the lifetime of the cable insulation. No unacceptable reduction of the breakdown strength will likely occur during this period. It is important to note that this depends on the insulation and material cleanliness of the cable core[16].

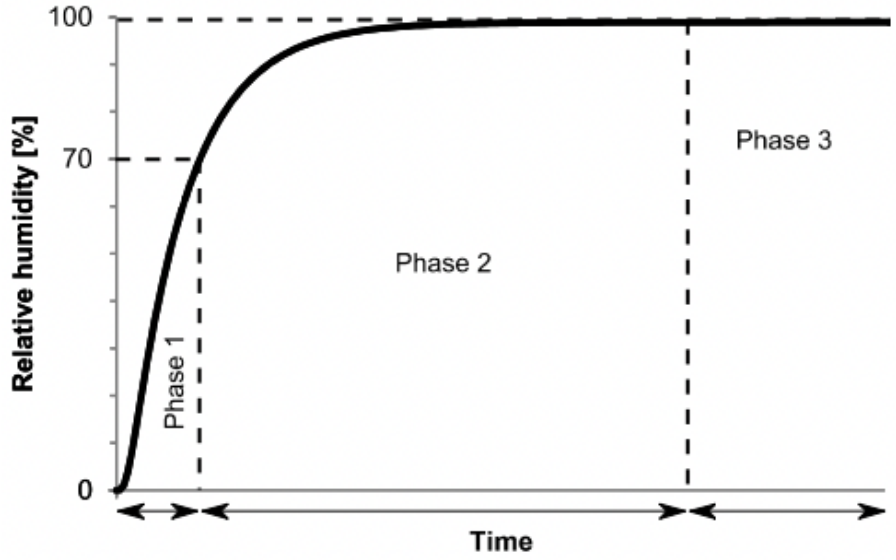

Figure 9: Humidity increase in the insulation of XLPE cable, where water absorption occurs from the outside[16]

2.2.6 The effect of mechanical stress on water tree growth in XLPE-cables

Previous research indicates that mechanical forces on the insulation influence the growth of water trees[4]. The theory behind the initiation of vented water trees is based on the presence of microscopic voids within the insulation. If the insulation is being stretched, these voids will expand, increasing the possibility of initiation of water trees and the growth rate[17].

After extrusion, stretch forces can develop in the insulation during the cooling process. This is due to the thermal expansion of the polymer. As the outer part rapidly cools down, shrinks and solidifies, the inner part of the insulation will cool down at a slower rate, which introduces internal stretch forces and causes compression of the outer surface. Compared to the conductor the polymer has a relative high thermal expansion capacity. Therefor the inner most part of the insulation can not shrink to the equilibrium dimension. Combination of these two mechanisms creates complex distribution of longitudinal, tangential and radial frozen mechanical stresses within the insulation. The longitudinal forces has been measured to be typically around 10-30 MPa, which can be higher then the yield strength of polyethylene. It is therefor possible to assume there are crazes present in the insulation and stretch stresses on the inner most part of the insulation, and compressive stresses on the outer most part[18]. During installation and under operation, the cable can be exposed to additional stresses by for example bending the cable, which can enhance growth of crazes.

2.3 Previous findings

The table below shows summarize of aging parameters used by earlier master's theses.

Table 1: The table summarizes the aging parameters used by some of the earlier master's theses and research articles

Study:	Aging parameters:	Amount of mechanical stress:	Aging time:	Temperature:	Voltage:
Virkning av mekanisk spenning på vanntrevekst i PEX isolerte høyspentkabler[17]. By: Simon Å. Aarseth. Year: 2013	Static mechanical tension Water in conductor	1%	3 and 4 weeks	Room temperature	13.85 kV 25 kV
Vanntrevekst i mekanisk og elektriskpåkjente PEX-kabler[6]. By: Truls A. Lindseth. Year: 2011	Static mechanical tension Water in conductor	28.9%	3, 6 and 9 weeks	30°C 60°C	13.85 kV
The Influence of Strain on Water Treeing in XLPE Power Cables[19]. By: Ståle Nordås and Erling Ildstad Year: 2010	Static mechanical tension	4% 5% 10% 17%	3 and 9 weeks	30°C	24 kV

S. Å. Aarseth concluded that forzen in forces which is formed close to the conductor increase occurrence of vented water trees at the inner semiconductor and the density of bow-ties. It was found that 5.6% frozen in forces can be released in axial direction by slowly cooling the insulation from 120 °C to room temperature. He also concluded

that the length of the vented water trees is shorter if the conductor is removed from the insulation, and the average maximum length of the bow-ties is not affected by the frozen in stretch forces. It was documented that the density of bow-ties is significantly lower in the outer part of the insulation compared to the inner part for cables with static mechanical stress applied. He also concluded that the growth of vented trees is about the same with and without the mechanical stress applied[17].

T. A. Lindeseth conlcuded that the stretch forces applied will increase the occurrence and length of bow-tie trees, compared to a cable with no mechanical stress applied. Compression forces applied will reduce the growth of water trees. This result applied to both 30 °C and 60 °C. Occurance and length of the vented trees was not affected by the introduction of static mechanical stresses with temperature gradient. T. A. Lindseth did find that combination of water in heated conductor and temperature gradient there was an increase in water tree length and occurance. He also documented that the maximum length of vented and bow-ties trees increase in length as a function of aging time and that there is increase in vented trees at 30°C compared to 60°C[6].

S. Nordås and E. Ildstad documented that there is a higher amount of vented water trees at the inner semiconductor with stretch forces applied despite that the mechanical force is higher at the outer semiconductor. However, the length of the vented trees found at the outer semiconductor is two times longer than those found in the inner semiconductor. It is documented that there was a increase in vented water trees found in the stretch zone compared to the compression zone. It was found that the the mechanical stresses influenced the occurence of bow-ties where 75% of the bow-ties was found in the sectors with stretch applied[19].

3 Method

The state of art and related work were reviewed, and an identification of the relevant background material were carried out in the project preceding this thesis[1]. Additional information was added to section: 3.3.3 microscope analysis, 3.4 Statistical presentation and 3.4.1 Estimation of maximum bow-tie tree length using extreme value statistics.

3.1 Test object

The test objects in this project are ten, 4 meters long, triple extruded XLPE-cables rated at 12kV. The cable consists of a $120mm^2$ copper conductor with 19 twisted strands. There is an inner conductor screen, insulation, and insulation screen, meaning it is a triple extruded cable.

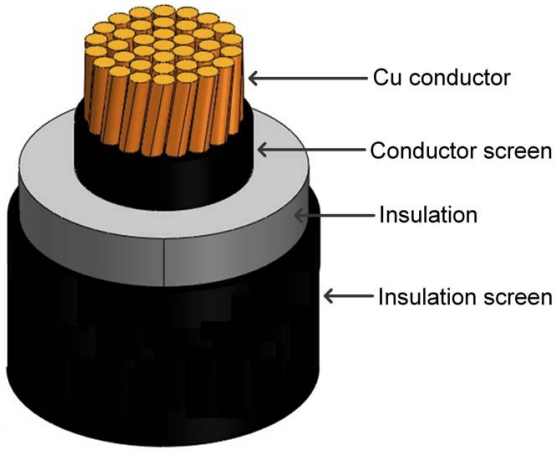

Figure 10: Illustration of XLPE-cable used [20]

The conductor screen is a semiconducting material made of carbon black blended with a polymer matrix. The screen's function is to smooth out any irregularities of the conductor and remove voids between the conductor and insulation surface. This inevitably provides a uniform divergent field within the cable core[21]. The insulation screen serves the same purpose. The cable insulation is cross-linked polyethylene.

Table 2: Cable dimension 12 kV, 120 mm2 Cu

Dimensions - Cold	**Conductor**	**Inner conductor screen**	**Insulation**	**Outer conductor screen**
Nominal diameter	13.0[mm]	15.00[mm]	22.20[mm]	24.20[mm]
Nominal thickness		1.00[mm]	3.6[mm]	1.00[mm]

3.2 Method execution

This section describes the method used to build the test rig.

1. Preparation of the cable sample:
   (a) Termination 3.2.1
   (b) PD-test 3.2.2
   (c) Static loading 3.2.3
2. Water bed and heating system 3.2.4
3. Preconditioning 3.2.5
4. Included components
   (a) Transformer 3.2.6
   (b) Coil 3.2.7
5. Finalizing the build process 3.2.8

Figure 11 shows the proposed setup for the static mechanical load. With the water temperature set to 40 °C, the voltage on busbar U_{AC} = 30 kV with 10 cables connected in parallel. The diameter of the tubes are as follows 10 cm, 20 cm, 30 cm. U_{AC} = 30 kV was chosen to get an average electric field strength of $E_{avg} = 5.35kV/mm$. The electric field strength closest to the conductor is $E_{max} \approx 7.43kV/mm$ and the electric field strength at the outer semiconductor is $E_{min} \approx 4kV/mm$.

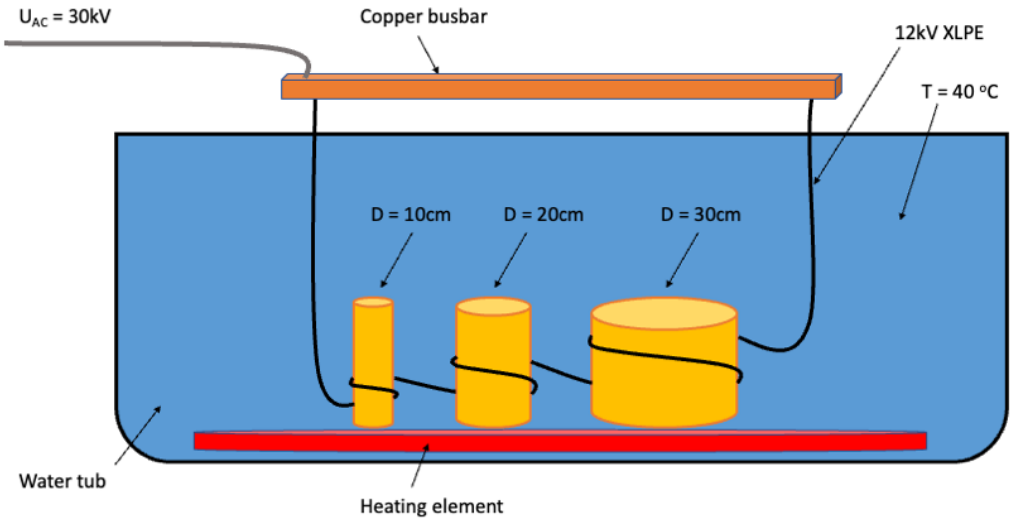

Figure 11: Sketch of setup

3.2.1 Cable termination

As seen in figure 12, the cables came in a raw state. The Cables were delivered in pieces of 4 meters each from the factory. The first order of action was to cut off 3 cm on each side of the cables with a saw to get a cleaner cut. The cables were cut using a cable cutter from the factory, which squeezed the ends. Squeezed conductor can lead to a poor connection between cable shoe and conductor.

It was also essential to check all the cables for manufacturing defects. One defect was found, as seen in figure 13, which is a hole in the insulation screen that goes into the conductor. This defect had to be removed.

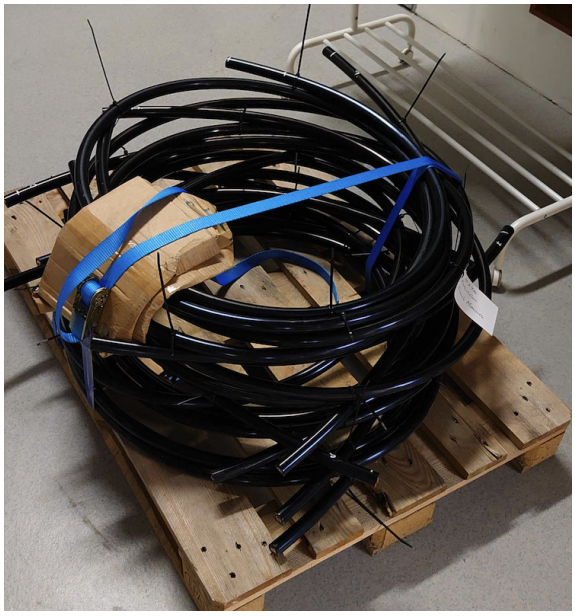

Figure 12: Cable in the state they were delivered

Figure 13: Manufacturing defect

The next part was to strip off around 30 cm of the outer insulation screen with an adjustable cable semiconductor stripping tool. At the cut-back point of the insulation shield, there will be an area of high potential gradients, which causes high electrical stress. Therefore, it is essential to be accurate with the knife to avoid sharp edges when the cut-back point is reached, as the sharp edges can lead to

higher electrical stress and air pockets. Because of this high electrical stress at the cut-back point, a stress control sheet must be added. The material is used to control and smooth out the electric field. As explained above it is crucial to get this sheet as tight as possible to remove any air pockets, without overstretching the material. Over this sheet, a self-fusing tape was also added. It serves the same purpose and adds an extra layer of security. The tape is marked with eclipses on the outside, turning into circles when stretched. These markings work as an indicator of the amount of stretch and force that needs to be applied. The last part that was done before PD-testing was adding a ground wire around the cable.

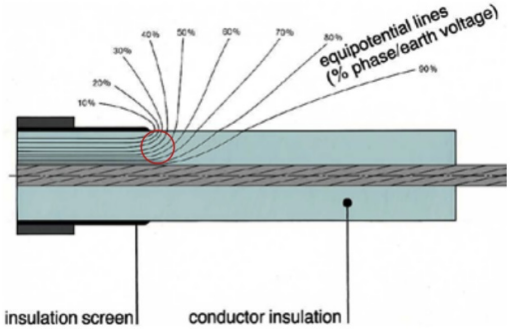

Figure 14: Cable end without stress control

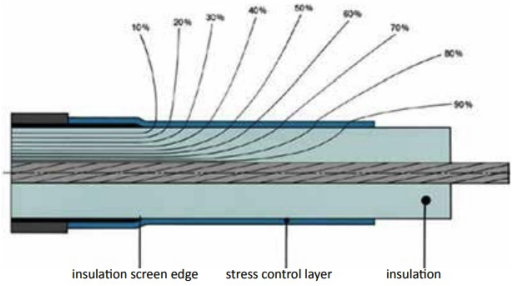

Figure 15: Cable end with stress control

Figure 14 shows how the equipotential lines are more concentrated at the cut-back point of the outer insulation screen without any stress control material, compared to when stress control material is added in figure 15

Figure 16: Stripping semiconductor

Figure 17: Adding stress control sheet

Figure 18: Picture of a breakdown in the termination

Figure 18 is a example of a breakdown in the termination. The cause of this breakdown probably is an air pocket between the stress control sheet and the insulation at the cut-back point.

3.2.2 PD-test

PD-measurement was done based on the measuring circuit in figure 19 using Omicron MPD600. C_k is a coupling capacitor, and the test object is connected in parallel. CPL542 is the measurement impedance with the possibility of measuring voltage over the test object. The MPD 600 advanced partial discharge measurement and analysis module are connected in parallel over the measurement impedance. There will be voltage drops in the circuit when there is PD activity. The coupling capacitor compensates for the voltage drop, and the compensation is measured over the measurement impedance.

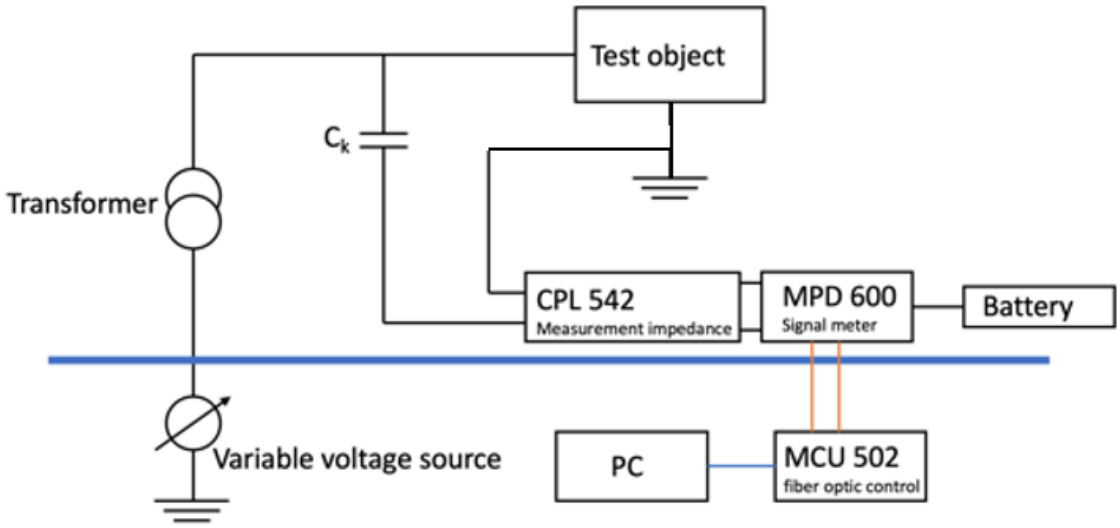

Figure 19: Measuring circuit

After the cable termination was complete, the cables needed to be tested for PD-activity. The test voltage was slowly increased to 36 kV to ensure each of the cable terminations could handle the operating voltage at 30 kV with some margin. As seen in figure 20, each cable was tested for 1.5-2 minutes, and 8 out of 10 cables passed on day 1 of testing.

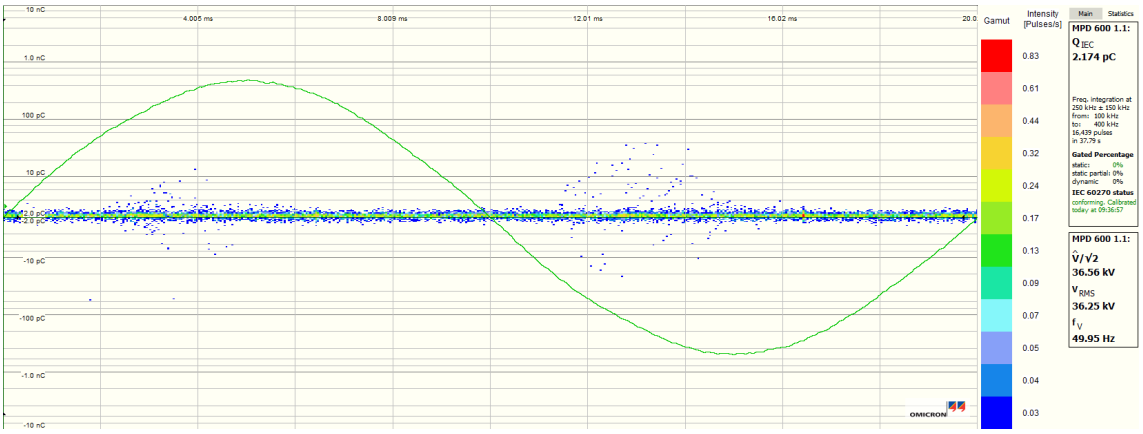

Figure 20: PD-test at 36 kV

The first cable that failed can be seen in figure 21. It is unsure why there was PD at 6.7 kV, mainly because it should not be any PD at this voltage level from the cable even without the termination. However, leaving the stress control sheet and tape to settle for a day and washing the termination with isopropanol worked, and the cable passed the test at 36 kV the next day.

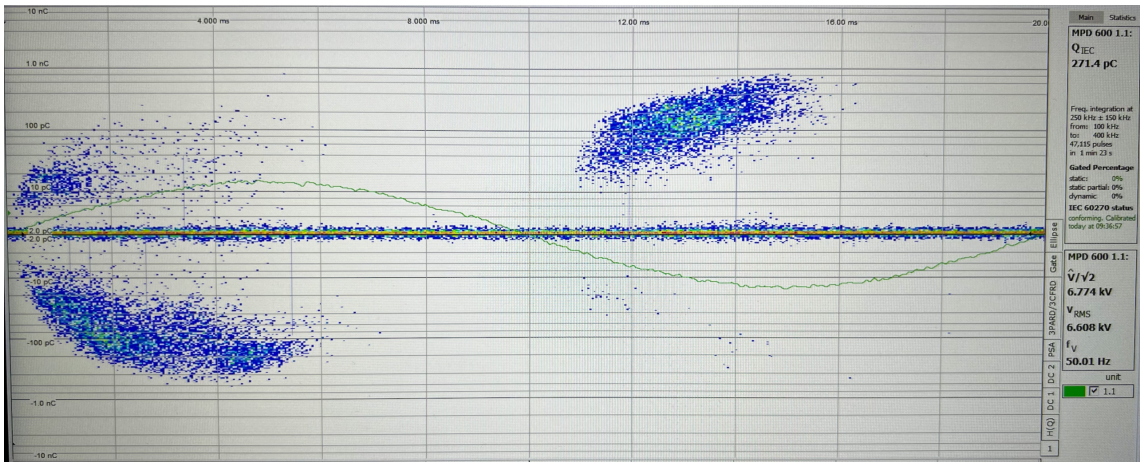

Figure 21: Cable failed PD-test at 6.7 kV

PD-test from the last cable that failed can be seen in figure 22. This cable failed at 23 kV, and based on the symmetrical appearance, this probably was because of air pocket in the termination. The air pocket most likely diffused overnight, as the cable passed the test up to 36 kV the day after.

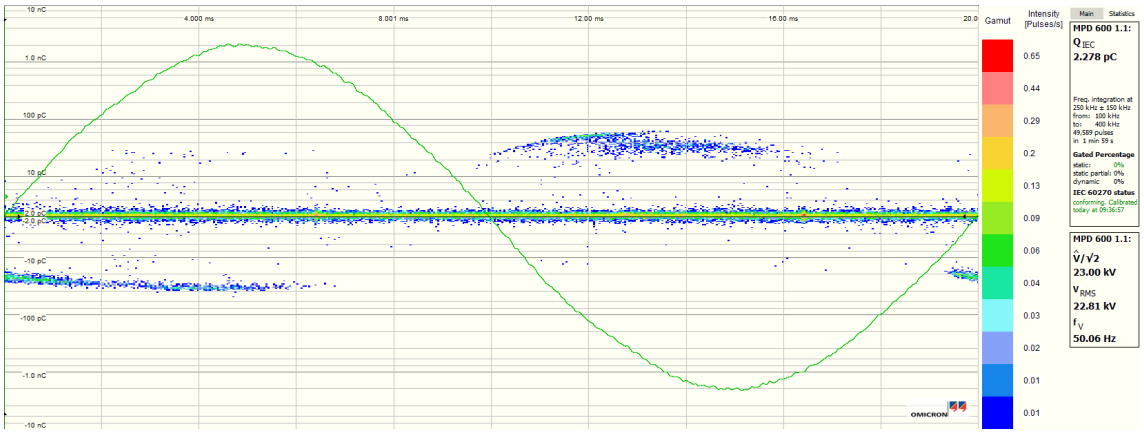

Figure 22: Cable failed PD-test at 23kV

3.2.3 Static mechanical load on cables

The cables were bent around three different pipes to induce axial static mechanical strain. The outer side of the cable will be stretched, and the inner side will be compressed. The amount of strain applied will vary dependent on the diameter of the pipes. The smaller the pipe, the larger the tension and compression. Some assumptions were made to calculate the diameter of the pipes needed to get the desired tension. The first assumption is that the cables follow Hooke's law and deform elastically. The second assumption is that there will be a neutral plane at 0°and 180°point where the strain will be zero. The axial strain can then be calculated with the formula 3.1[19].

$$\epsilon_z(r,\theta) = \frac{\Delta l}{l} = \frac{2rsin\theta}{D_C + 2r_O} \tag{3.1}$$

where D_C is the cylinder diameter, and r_O is the outer diameter of the cable, which gives a good illustration of the distribution of the strain based on angular position.

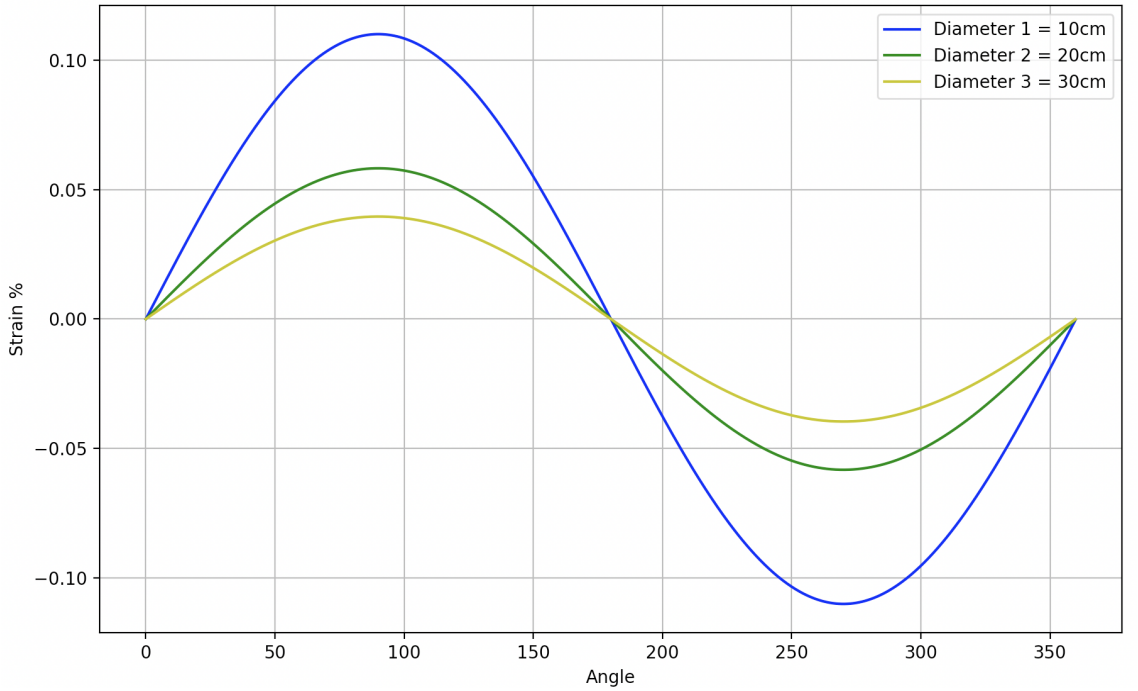

Figure 23: Estimated strain in % based on the angular position

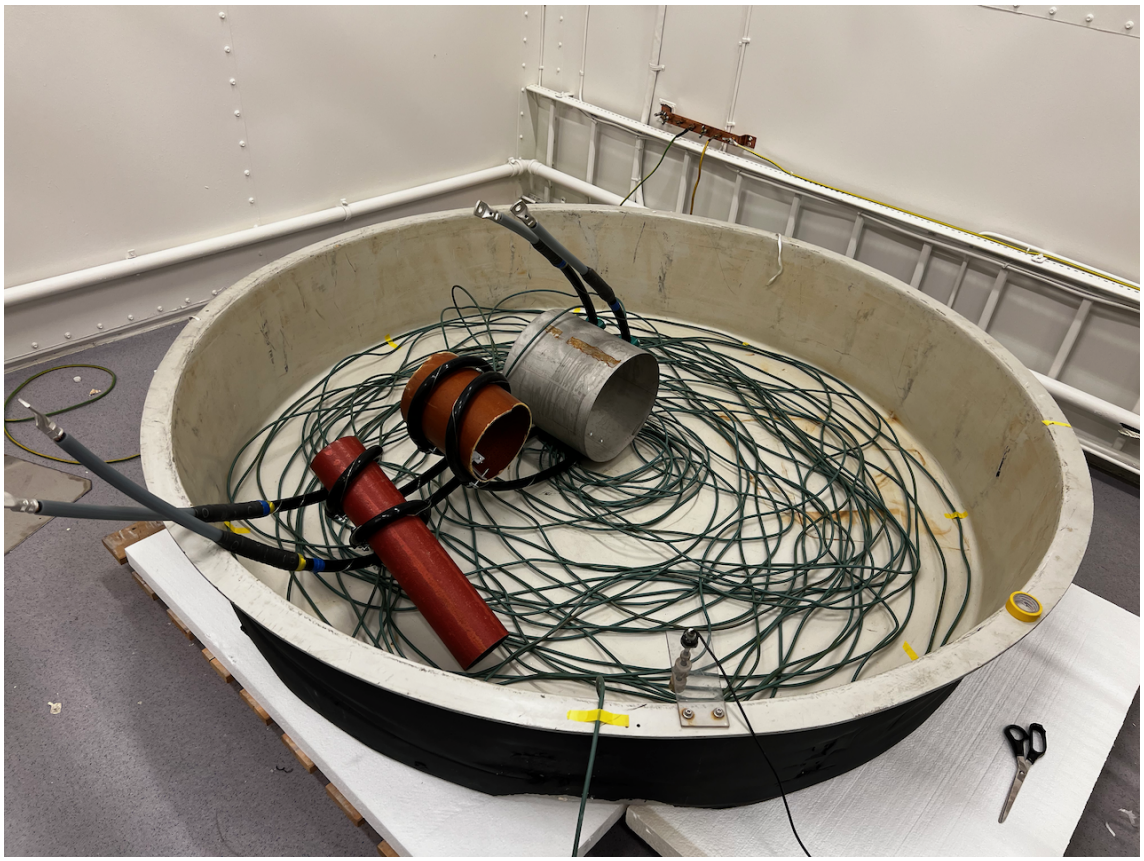

Figure 24: The first cable bent around pipes with 3 different diameters

The process of bending the cables around the pipes was proven to be more difficult than anticipated. Therefore the original idea of using four pipes with different diameters was axed. The smallest pipe at only 5cm in diameter would not be possible with the equipment available. To start with, the pipes were fastened to a table. The cables were then fastened to the pipe with cable clamps. Then a crane was used to bend the cable around the pipe, which again was fastened to the pipe with new cable clamps. The smallest pipe was made of iron, and therefore there were no worries about the high forces needed to bend the cables around the pipe. However, the middle pipe was made of wood and much more fragile, and after the some of them fractured it was clear the wooden pipe needed structural support. This was done with duct tape and a load strap. The challenge with the last pipe was that it was made of acid-proof steel, which is much harder then regular steel. Therefore, it was needed to predrill the holes before fastening the cables with clamps. The cables were bent around one turn with the two smallest pipes and 1/3 turn on the largest pipe. This ensures long enough test objects. A straight section of approximately 15cm between the smallest and the middle pipe was also added in case there is interest in testing a section with no mechanical stress.

3.2.4 Water bed and heating system

The water bed is 2 meters in diameter, 30cm in height, and holds around 940 liters. The heating system consists of a heater cable of 2100W and a temperature

controller unit. Connected to the temperature controller are the primary target temperature sensor and a secondary temperature sensor which will cut power if the water temperature goes above a given temperature. There is also a fire alarm and water level sensor. The water level sensor has two stages. The first stage gives an alarm if the water goes below the first stage, and the second stage will cut power to the heater cable.

Figure 25: Temperature controller

Figure 26: Water level sensor

3.2.5 Preconditioning

The cables need to be preconditioned before voltage can be applied to the test objects. The table Nexans provided below does not include this specific cable. However, the insulation thickness is more or less in the middle of cable number 1 and 2, making the preconditioning time around 400 hours at 55°C, or 16.5 days. Due to delays in the building process, the cables were allowed to precondition for 23 days, or 552 hours at 55°C, meaning the cable should have an relative humidity value of at least 96% according to table 3.

Table 3: Conditioning time provided by Nexans

Cable no.	Test(s)	Cable rated voltage	$T = 55°C$		$T = 70°C$		$T = 90°C$	
			$t_{95\%RH}$	RH_{500h}	$t_{95\%RH}$	RH_{500h}	$t_{95\%RH}$	RH_{500h}
			[h]	[%]	[h]	[%]	[h]	[%]
1	2-1, 3a	12 kV	320	99	85	100	18	100
2	2-2	12 kV	473	96	128	100	28	100

During the beginning of the preconditioning of the cables, it was clear that the heating element alone would not suffice to get the temperature up to 55°C due to the high surface area. Even if it could, the evaporation rate would be high, and the water bed would constantly be needed refilling. That is why the area underneath the water bed was insulated with polystyrene, insulation material around the water bed and the water surface area was insulated with bubble plastic, as shown in figure 27. The cable termination needed to be kept above water and preferably above the bubble wrap so that moisture would not enter the terminations. This is because

the terminations are only PD-tested under dry conditions and thus will have less control over the strength of the termination if they get wet.

Figure 27: Polystyrene insulation at the bottom, insulation material around the water bed and bubble plastic at the water surface

3.2.6 Transformer

The first meeting with Nexans concluded that the cables should be put through a high aging gradient. In this case, at around 10kV/mm. This is done by 30kV induced voltage. One challenge was finding a transformer that could handle 30kV and the load current drawn by the cables. One thing is finding a transformer that could handle this load. Another is to find a transformer that can handle it under sustained load. The transformer used is an oil-cooled 3-phase distribution transformer coupled in 1-phase. The transformer can deliver 30kV at 0.77 amp, as seen in figure 28 of the nameplate below. The turn ratio of the transformer is $\alpha = \frac{30000V}{220V} = 136.36$.

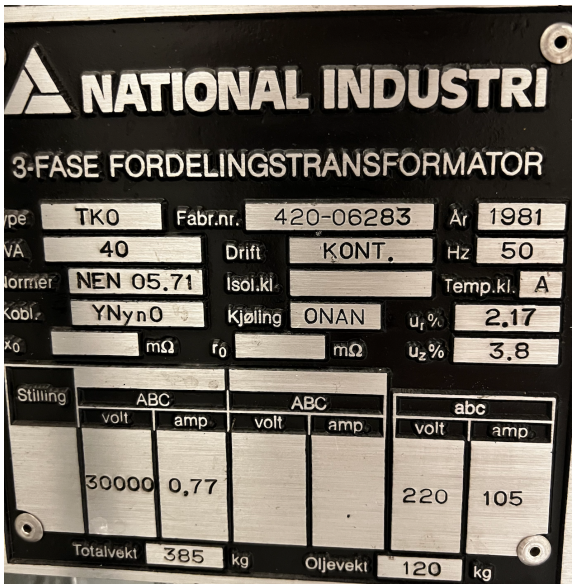

Figure 28: Nameplate of transformer with specifications under sustained load

If obtaining one large enough transformer would be difficult, it could have been solved by using two smaller transformers instead. However, to ensure a more even aging gradient on all the cables, it was preferred to use only one.

3.2.7 Coil

With around 35 meters of cable connected to the system, there was a concern that the high capacitance in the cables would pull too much current from the grid.

Figure 29 shows the nameplate of the coil with an inductance of 10.3mH. The coil should ideally have been connected in parallel. However, the nameplate of the coil does not say anything about the voltage it can tolerate, and the datasheet was not possible to obtain. Therefore the coil was connected in series. It will consequently compensate to a lesser extent for the capacitive current. However, it will act as a filter for the current and voltage. There is harmonic resonance in the current without the coil, as seen in figure 30. This happens because the current delivered from the grid is not clean sinusoidal and resonates with the system's natural frequency. The coil moves the system's natural frequency thus removing harmonic resonance, as seen in figure 31. It is crucial to remove harmonic resonance from the system, especially on the voltage, as the terminations are increasingly susceptible to degradation from harmonic stresses.

Figure 29: Nameplate of coil

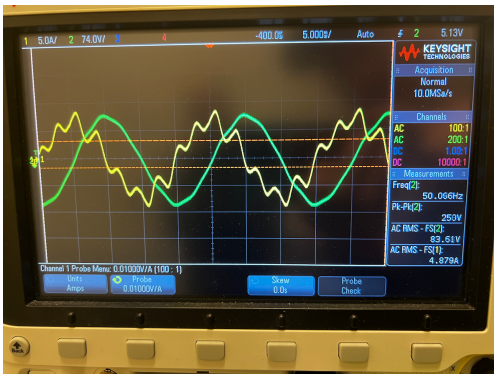

Figure 30: Without coil connected, the green signal is voltage and the yellow signal is current

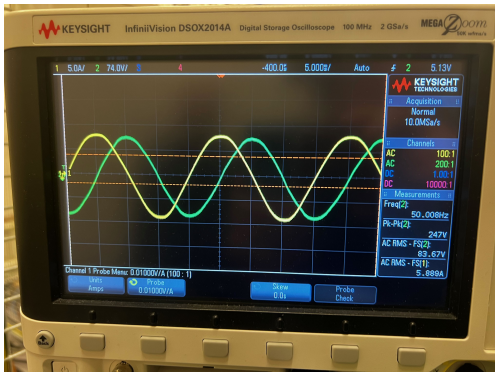

Figure 31: With coil connected in series

3.2.8 Building process

The next part is to connect everything. The busbar was placed on two insulators in case the wood it stands on would get conductive due to moisture. All the cables were connected to a copper busbar in parallel using copper tubing. At this point, it was essential to choose tubes that were at least 1cm in diameter. By using tubes with smaller curvature there is a good chance of getting PD from the tubes or connections. It was also essential to ensure that there were no sharp points in any of the critical parts of the build. This is why the screws connecting the copper tubing and cables had to be trimmed down. The busbar was connected to the transformer using a larger aluminum tube.

The transformer was coupled as 1-phase and connected to the coil, which again was connected to the voltage regulator. The entire setup can be seen in figure 33, with the equivalent circuit shown in figure 32. Note that the equivalent circuit shows the measured value for current, the delivered voltage from the source, capacitance of the cables and inductance and resistance neglected.

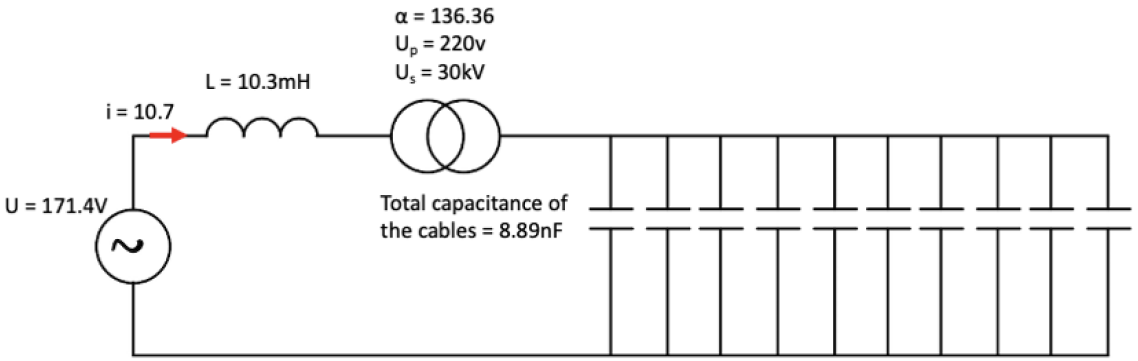

Figure 32: Equivalent circuit of the complete setup.

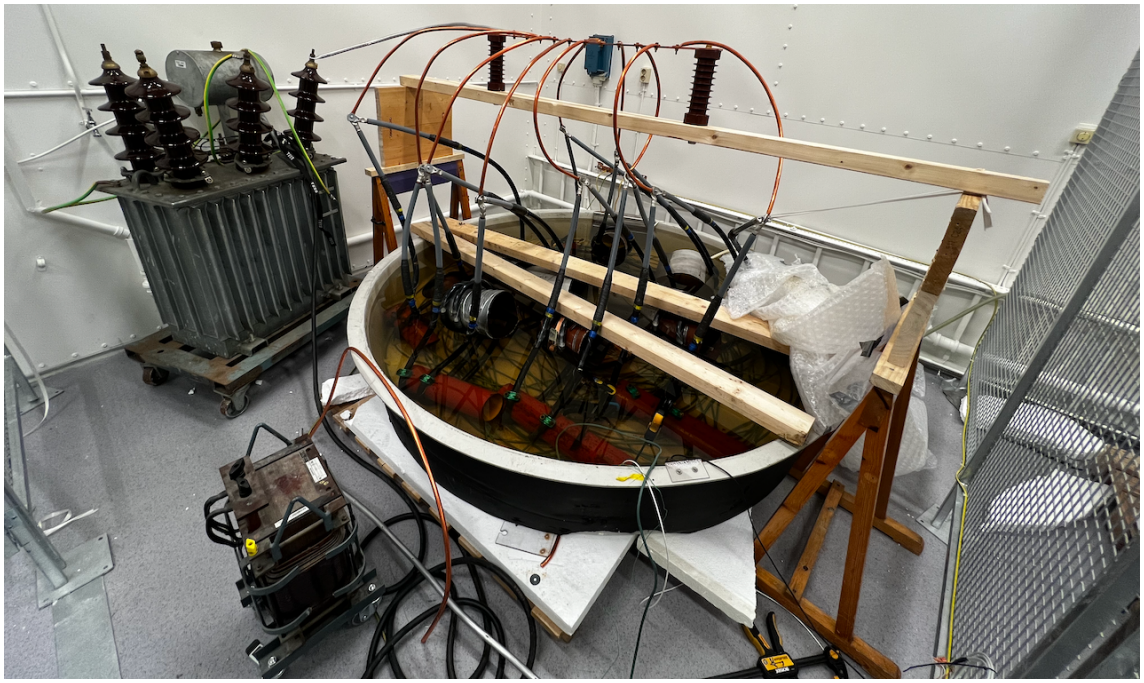

Figure 33: Complete setup

3.3 Microscope Analysis

Each of the test objects was aged at 30kV resulting in a field strength of 10kV/mm at 40°C. After 30 days, the first cable was disconnected and inspected using the procedure described below. The rest of the test objects followed the same time steps of 30 days, giving a maximum aging time of six months. By following this timeline, six cables was tested over this period, which gave room for four cables to fail during the aging process without disrupting the timeline.

3.3.1 Preparation of cables for microscope analysis

The cables was cut into 10 cm pieces. The pieces represent the area where the mechanical tension and compression were the highest at each pipe.

A small cut in the insulation screen was made to distinguish where the cable was subjected to tension and compression. The cut was made with a special cutting tool at the area of highest compression as shown in figure 34.

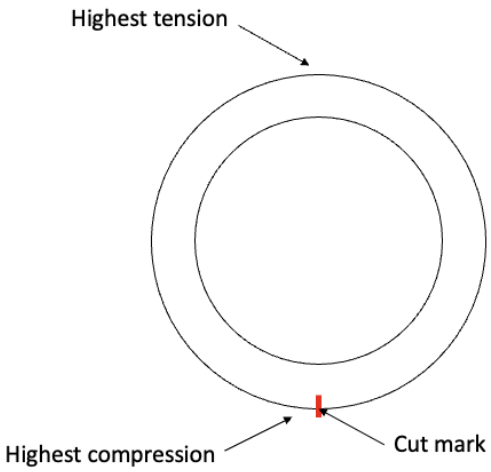

Figure 34: Illustration of cut-marks in the cable

The next part was to remove the conductor from the insulation. This was done by connecting one clamp to the conductor, one to the insulation and by using a crane, pulling the conductor out of the insulation.

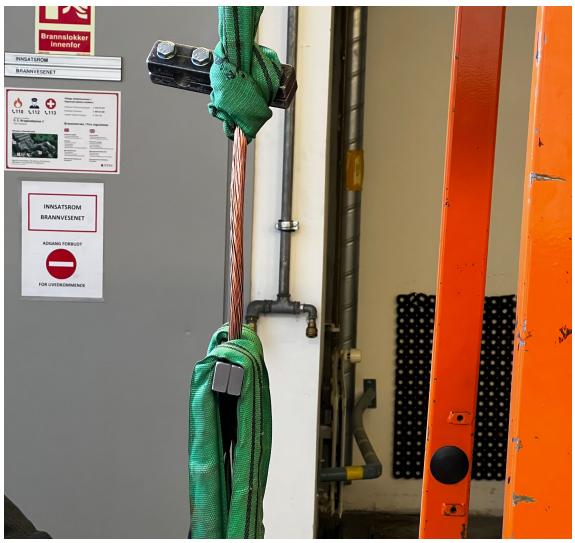

Figure 35: Conductor being pulled out of the insulation using a crane.

The next step was to cut the insulation helically using a rotary knife. The insulation was cut with a thickness of 0.5mm and attached to steel wire as shown in figure 36

Figure 36: Picture of helically cut insulation.

3.3.2 Dyeing

The next step was to dye the insulation. This makes it easier to see the water trees under the microscope. This was done following the standard Cigre-dyeing method. It will be used a mixture of methylene blue, Sodium carbonate and water. ingredient quantities are presented in the table 4 below:

Table 4: Ingredient's list for the coloring mixture

Ingredients	**Quantity**
Methylene Blue	6 g
Na_2CO_3	0.5 g
Water	200 ml

The solution are mixed in a flask with magnetic stirrers in a heating cabinet. The temperature was set to 67.5°C, and the mixture was be stirred for a minimum of 5 hours. After 5 hours the stirring was stopped, so that the mixture could settle for 20 hours in the heating cabinet. The mixture was then again stirred for another hour. At this point, the mixture is ready, and the helicoids of insulation was fully submerged for around 5 hours. The solution can be used up to 6 times before a new batch needs to be made. However, each time it is reused, the helicoids need to be submerged for a longer time as the dye loses color. The longer it is submerged, the darker and more concentrated the dye.

3.3.3 Microscope analysis

Each of the helicoids was cut into circles and cleaned with isopropanol to remove excess dye. It was then used dimethyl phthalate to smooth out the surface of the sample.

From each helicoids there was at least ten samples inspected. It was then documented the length of the longest bow-tie in each of the two zones. The size and location of vented water trees was also recorded, if found. In some cases the source of the vented water tree was also visible and therefor documented.

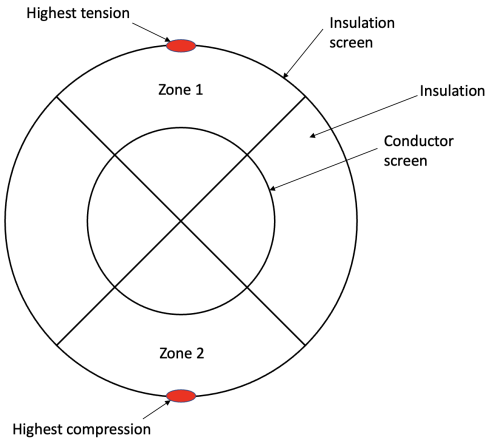

Figure 37: Illustration showing how the zones are divided

3.4 Statistical presentation

As explained in section 2.2.4, long water trees can reduce the breakdown strength of the cable and at the same time reduce the expected lifetime. Usually vented trees are the primary source of a breakdown in a cable, however bow-ties can also be a contributor to breakdowns if the density and length is sufficient in size.

Due to the quality of the XLPE-cable there was limited growth of vented trees, at least not enough to get a good statistical basis for reliable results. However, the results from the vented trees can be used as a guidance for this specific type of cable under similar conditions. There was however sufficient growth of bow-ties to get a statistical basis. The results of this thesis is therefor focused more on the statistical analysis of bow-ties.

3.4.1 Estimation of maximum bow-tie tree length using extreme value statistics

The results is presented first and foremost using Weibull probability plots. This was done using Matlab and the wblfit function which returns the estimates of Weibull distribution parameters (shape and scale). Minitab was used to compose the plots presented in the results. This was done as the plots Matlab returned using wblplot function, did not match the data from the wblfit function.

The wblfit function uses two simultaneous equations to find the maximum likelihood estimators $\hat{\eta}$ and $\hat{\beta}$ from the η scale and β shape parameters seen in the equations below. These two maximum likelihood estimators are the parameter that maximize

the likelihood function for fixed values of x. In this specific case x is the longest bow-tie from each test sample and n is the amount of test objects.

$$\hat{\eta} = \left[\left(\frac{1}{n} \right) \sum_{i=1}^{n} x_i^{\hat{\beta}} \right]^{\frac{1}{\hat{\beta}}} \tag{3.2}$$

$$\hat{\beta} = \frac{n}{\left(\frac{1}{\hat{\eta}} \right) \sum_{i=1}^{n} x_i^{\hat{\beta}} \log x_i - \sum_{i=1}^{n} \log x_i} \tag{3.3}$$

Minilab works in the same way as matlab when it comes to compose the plots. It uses these likelihood parameters to calculate the cumulative distribution function of the Weibull distribution which is:

$$p = 1 - e^{-\left(\frac{x}{\eta} \right)^{\beta}} \tag{3.4}$$

The shape and scale parameters η and β from the wblfit function in Matlab was confirmed to be correct by the Minilab software.

4 Results

The results found by following the methodology in chapter 3 will be presented in this section. First follows the results from the bow-tie study. The subsections are divided into maximum stretch, minimum stretch, maximum compression and minimum compression. In each subsection, the Weibull probability plot comes first, then follows a plot presenting the scale parameter β development over time, and then the development of L_{max} and shape parameter η over time. The data used to make the plots can be found in the attachments.

In section 4.3, the results from the vented trees are presented to compare the number of observed trees in the stretch zone and the compression zone. Then follows pictures with description of the two largest vented trees that was inspected closer to find the cause of initiation.

Only the results from maximum and minimum mechanical forces applied will be presented. The results from the third, fourth, and fifth months of aging with medium mechanical force applied gave incorrect results and thus rejected, which is explained further in 5.3

4.1 Development of length of the bow-tie trees from one month to six months of aging with stretch applied.

In this subsection the results from the maximum stretch, minimum stretch, maximum compression and minimum compression will be presented.

4.1.1 Maximum stretch applied (12%)

Figure 38 illustrates the development of length of the bow-tie trees from one month to six months of aging with maximum stretch applied. The 63% line is the scale parameter η, which represents the average value of the cumulative distribution function. As seen in the figure, the η is increasing fast from the first month to the third month. With very small $\Delta\eta$ between the test objects after the third month of aging. The low $\Delta\eta$ between each month indicates that the growth of the bow-ties has started to settle. The shape parameter β has a decreasing trend. This means that the spread is increasing, resulting in a higher probability of finding larger bow-ties. At the worst case with five months of aging there is a 95% chance of finding a bow-tie that is 170 µm or smaller. The development of β over six months is illustrated in figure 39.

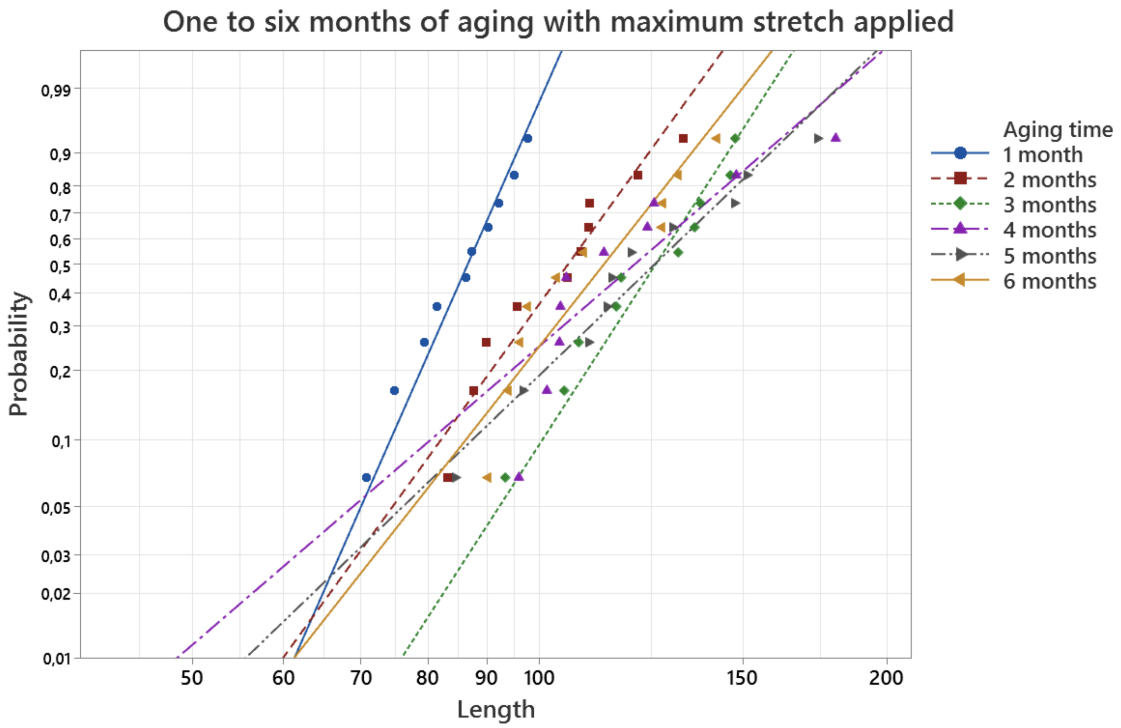

Figure 38: one - six months of aging with maximum stretch presented in Weibull probability plot

Table 5: Summarize of the η and β values from figure 38. Where the L_{max} value is the average length of the two longest bow-tie trees.

Maximum stretch			
Aging time	η (63% length)	β	L_{max}
1	89.26	12.27	96.42
2	111.23	7.46	127.38
3	131.79	8.37	147.18
4	130.85	4.65	164.45
5	135.06	5.20	162.65
6	119.87	6.86	137.23

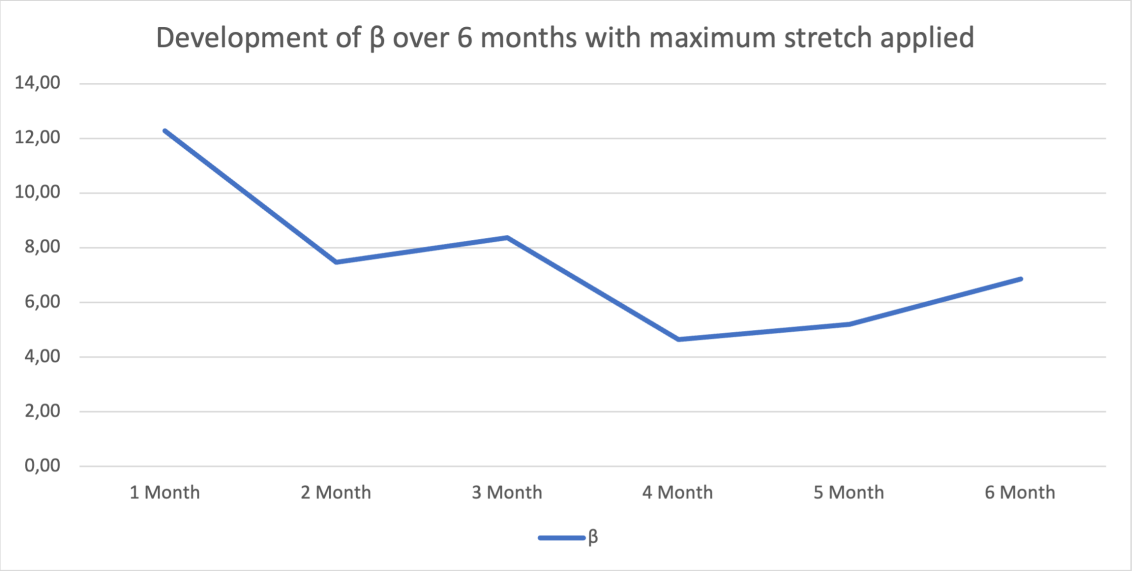

Figure 39: Development of β over 6 months with maximum stretch applied

Figure 40 illustrates the L_{max} and η over six months of aging. L_{max} and η increases with the same rate the first three months. However, η halts from the third month and out, and L_{max} continues the same increase for another month before it flattens out.

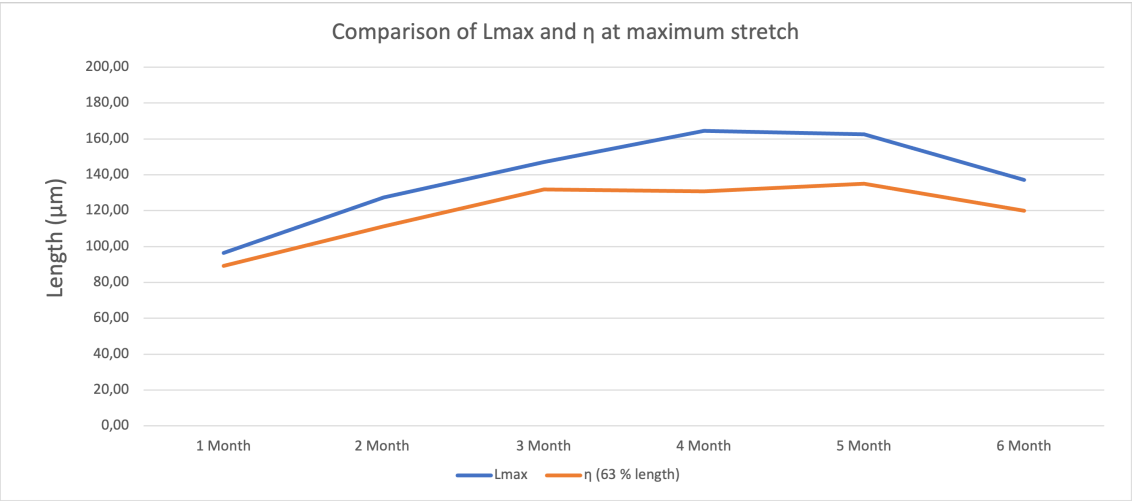

Figure 40: Comparison of L_{max} and η at maximum stretch vs. aging time

4.1.2 Minimum stretch applied (4%)

As seen in figure 41 with minimum stretch the β is more stable compared to maximum stretch with the exception of the third month which had one extreme bow-tie. This resulted in a very low β of 3.51 and a worst case scenario of 95% chance of finding a bow-tie that is 175 µm or less. However, the β value at 6.38 from the fifth month gives a better indication of the condition of the cable, and results in a 95% chance of finding a bow-tie tree with 155 µm in length or less. Figure 43 shows the same trend as in maximum stretch where the η increases rapidly the first three months and then tapers off.

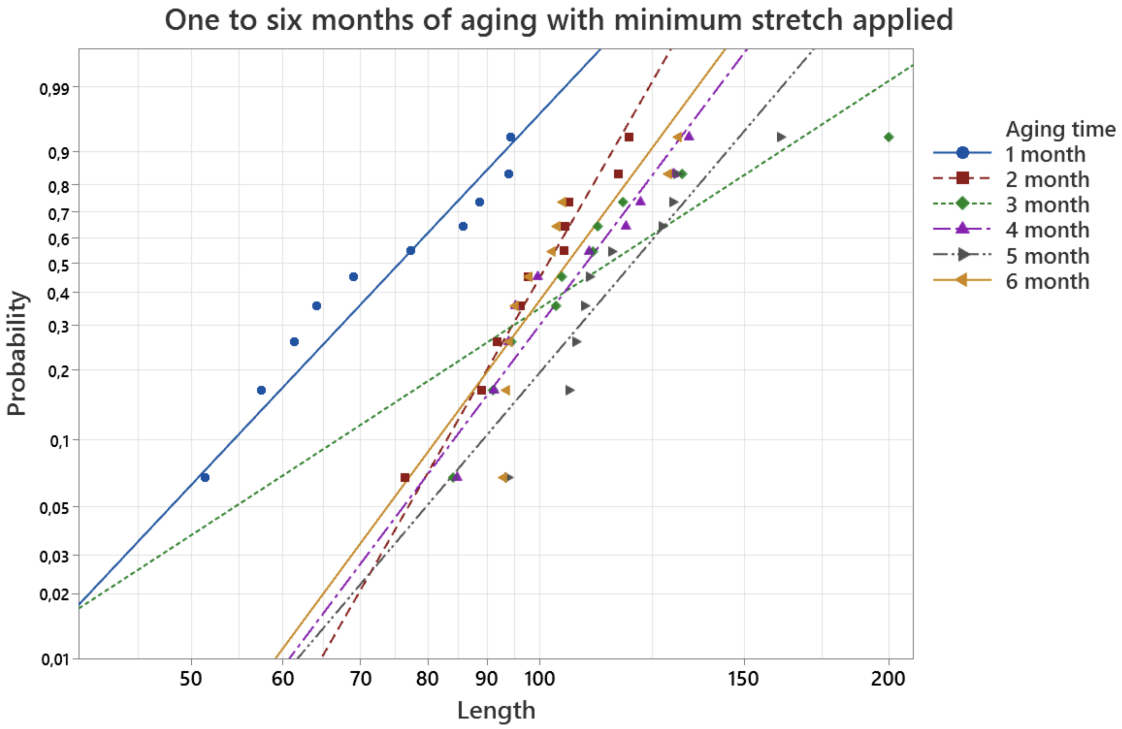

Figure 41: one - six months of aging with minimum stretch presented in Weibull probability plot

Table 6: Summarize of the η and β values from figure 41. Where the L_{max} value is the average length of the two longest bow-tie trees.

Minimum stretch			
Aging time	η (63% length)	β	Lmax
1	80.55	5.75	94.17
2	105.67	9.42	118.04
3	127.19	3.51	166.50
4	115.36	7.20	132.43
5	127.25	6.38	146.15
6	110.88	7.32	130.42

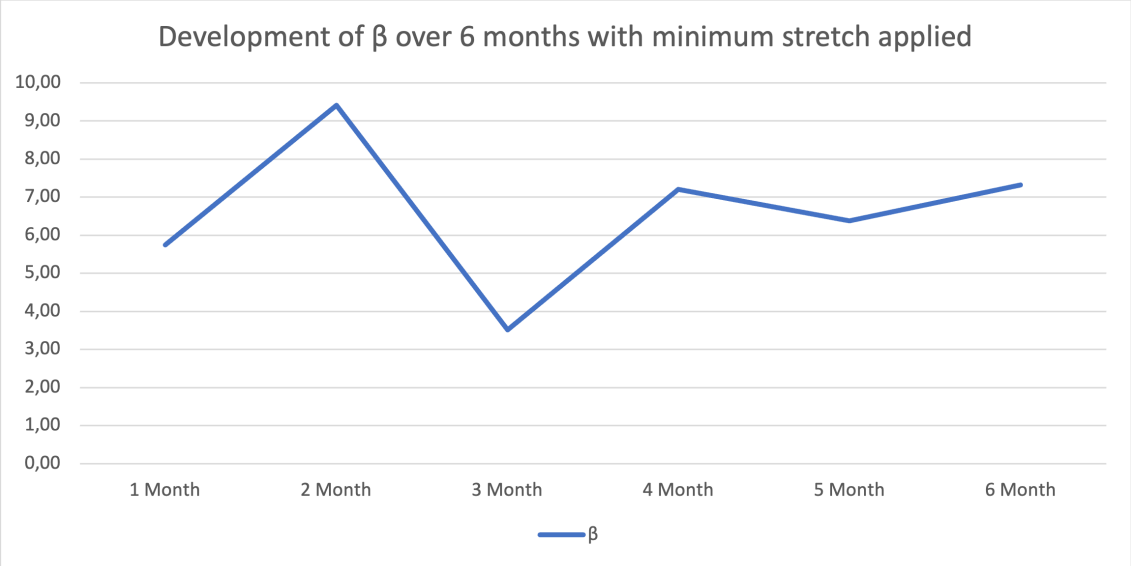

Figure 42: Development of β over six months with minimum stretch applied

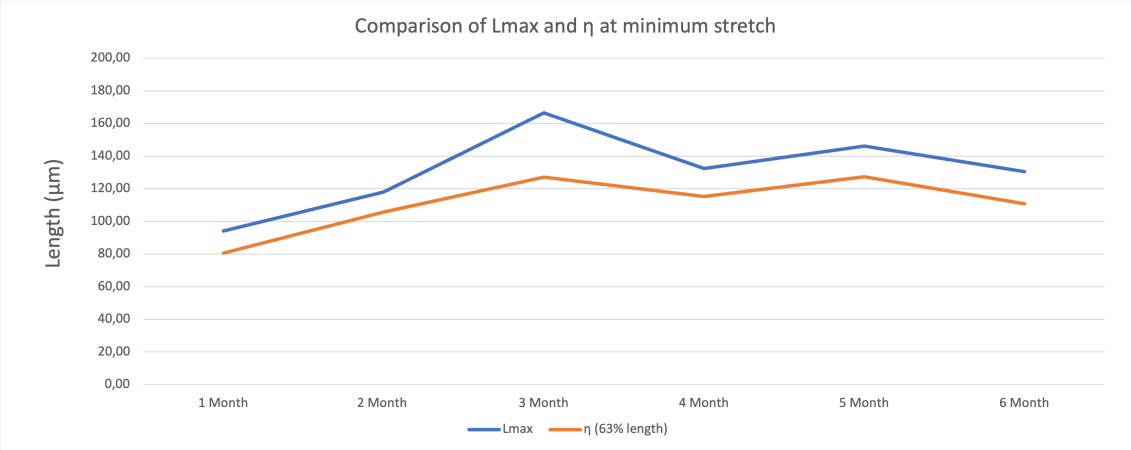

Figure 43: Comparison of L_{max} and η at minimum stretch vs. aging time

4.2 Development of length of the bow-tie trees from one month to six months of aging with compression applied.

In this chapter the results from the maximum (12%) and minimum (4%) compression zone will be presented.

4.2.1 Maximum compression applied (-12%)

Figure 44 illustrates the development of the length of the bow-tie trees from one month to six months of aging with maximum compression applied. As seen in this figure, the β is lower than in the stretch zone indicating worse condition in the compressed zone. Figure 46 shows that the η follows the same growth pattern as in maximum and minimum stretch.

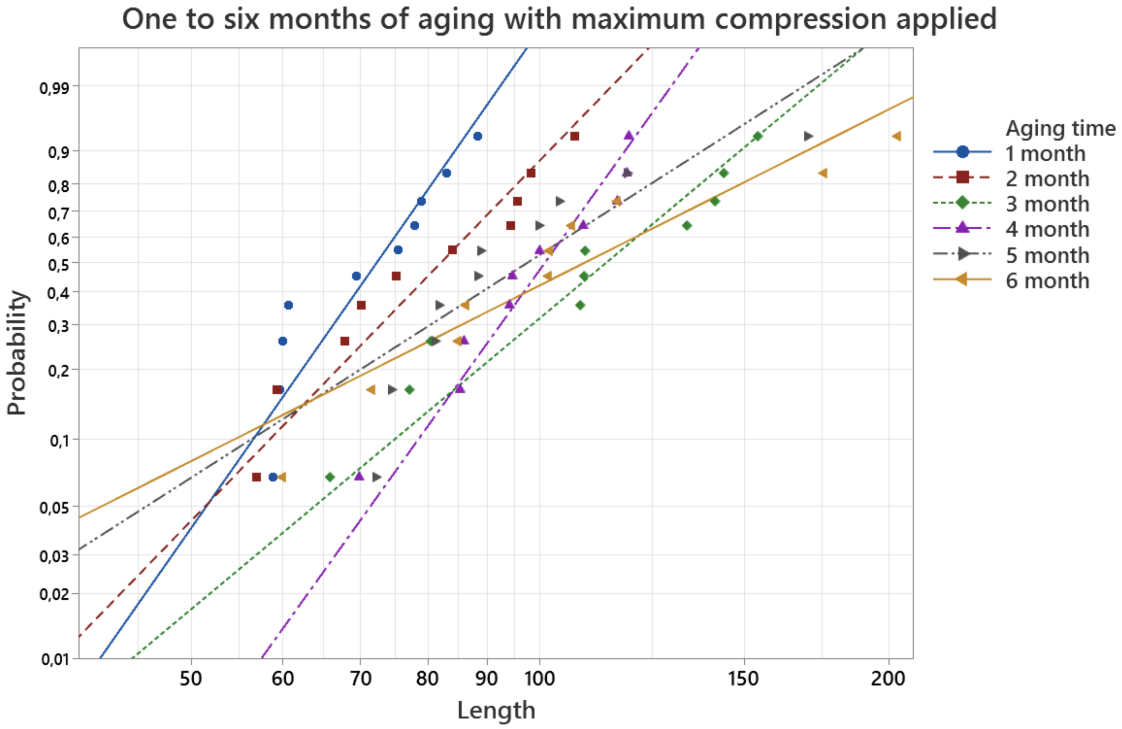

Figure 44: one - six months of aging with maximum compression presented in Weibull probability plot

Table 7: Summarize of the η and β values from figure 44. Where the L_{max} value is the average length of the two longest bow-tie trees.

Maximum compression			
Aging time	η (63% length)	β	Lmax
1	75.80	7.71	85.66
2	87.72	5.57	102.70
3	123.73	4.51	149.27
4	106.05	7.54	119.10
5	103.56	3.24	137.12
6	124.92	2.72	189.67

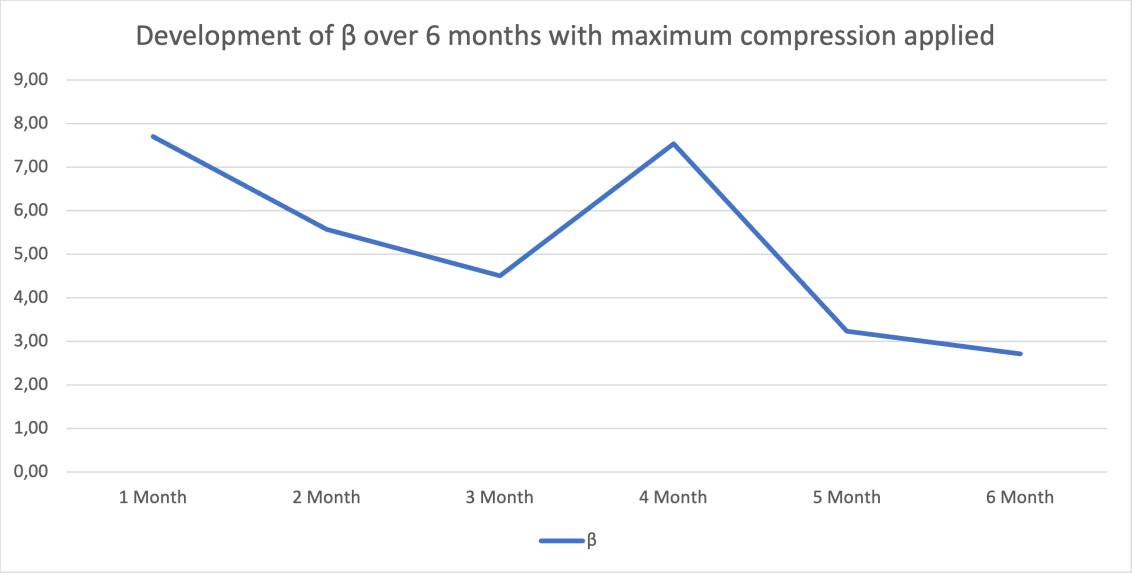

Figure 45: Development of β over six months with maximum compression applied

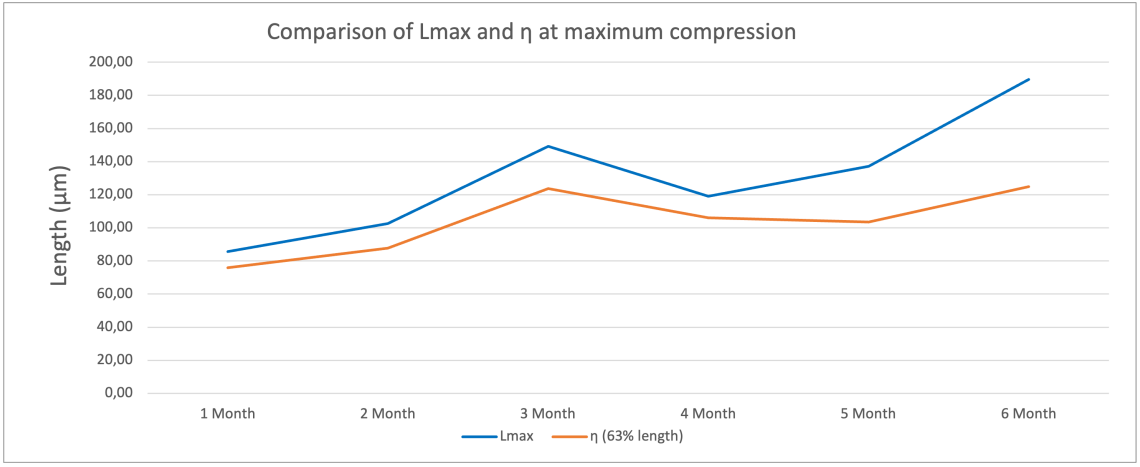

Figure 46: Comparison of L_{max} and η at maximum compression vs. aging time

4.2.2 Minimum compression applied (-4%)

Figure 47 shows that the β is very stable, indicating that the cable condition is not getting worse during the aging time of six months. η in figure 49 shows that the growth rate of the minimum compression zone is slower than maximum stretch, minimum stretch and maximum compression.

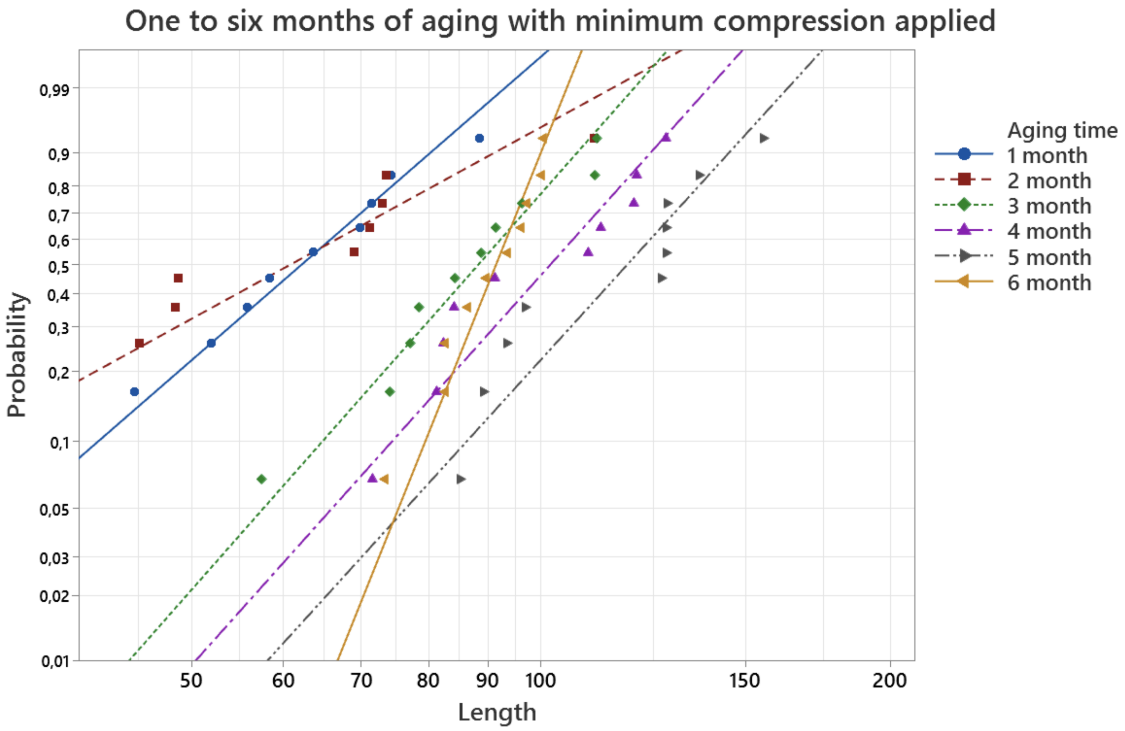

Figure 47: one - six months of aging with minimum compression presented in Weibull probability plot

Table 8: Summarize of the η and β values from figure 47. Where the L_{max} value is the average length of the two longest bow-tie trees.

Minimum compression			
Aging time	η (63% length)	β	Lmax
1	67.22	4.70	81.42
2	68.77	2.96	92.39
3	93.77	6.13	111.54
4	108.29	6.04	124.65
5	126.25	5.95	146.19
6	93.97	13.50	100.30

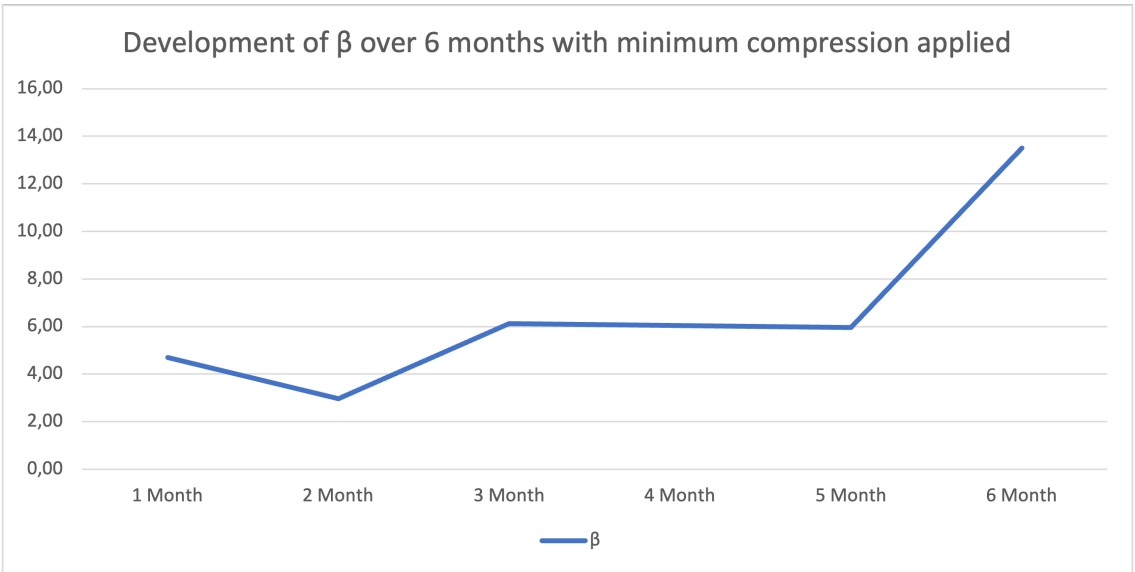

Figure 48: Development of β over six months with minimum compression applied

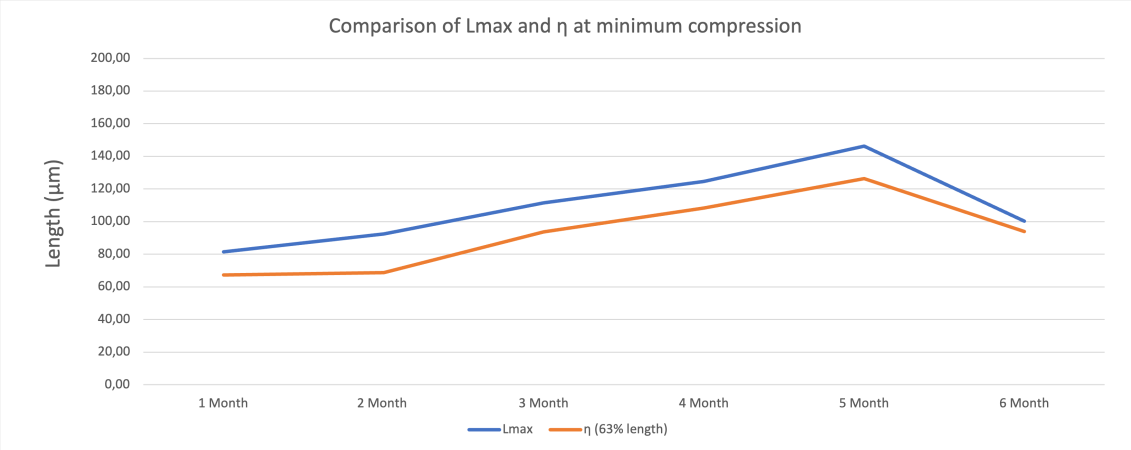

Figure 49: Comparison of L_{max} and η at minimum compression vs. aging time

4.3 Development of vented trees with applied stretch and compression forces

Table 9 and figure 50 show the distribution of all vented trees observed during the six months of aging. In order to improve the statistical significance, the tree count in maximum and minimum stretch was combined, so was maximum and minimum compression.

The vented water trees are distributed evenly across the stretch and compression zone. Only a single water tree was observed at the outer semiconductor; the rest was observed at the inner semiconductor. Most of the vented trees were observed in the parts of the cable with the least amount of static mechanical force applied (minimum stretch and minimum compression). As seen in figure 51 the η length of the vented trees in stretch zone was 80 µm in stretch zone, and 86 µm in the compression zone. The β is also a bit lower in the compression zone indicating worse condition there compared to stretch zone. The largest vented tree found was 250.1 µm, located in the compression zone.

Table 9: Amount of vented water trees observed over six months of aging.

Inner semiconductor	
Stretch	13
Compression	16

Outer semiconductor	
Stretch	0
Compression	1

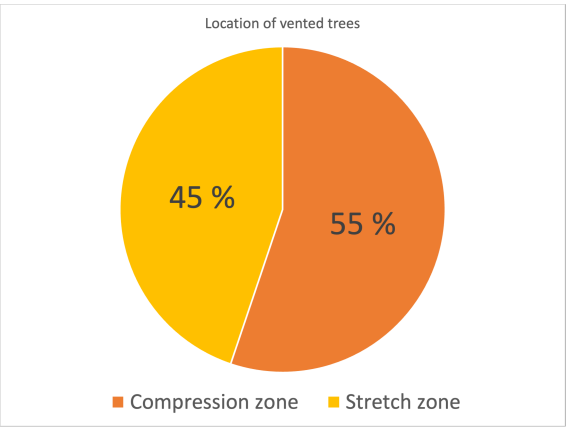

Figure 50: Distribution of vented trees observed at inner semiconductor during 6 months of aging

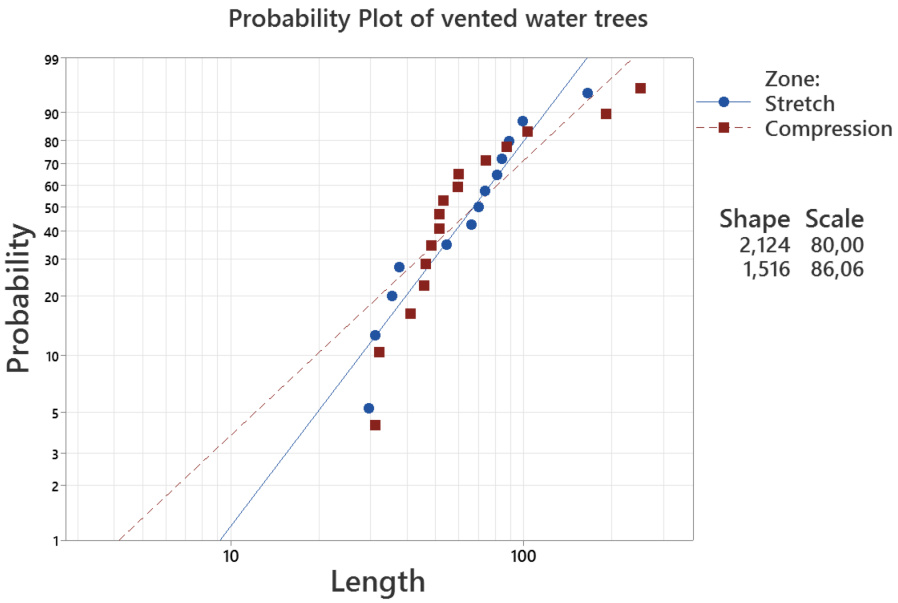

Figure 51: Weibull probability plot of the vented trees observed in stretch and compression zone

Figure 52 shows the largest vented tree found, with a length of 250 µm. The magnification setting on the microscope used to take the picture was 20x. It was inspected further under another microscope with magnification at 1000x. However, no unevenness was found that could be the cause of initiation. An attempt was made to tilt the microscope 45 degrees to see into the wall of the semiconductor without success. Therefor it was concluded that the most likely reason for initiation is a trapped particle or damage to the semiconductor that is not visible from above or below.

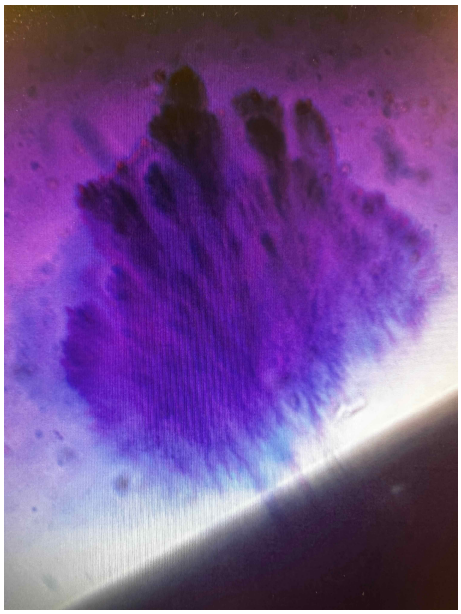

Figure 52: Picture of the largest vented tree found. Length = 250 µm from the cable that was aged for five months. Located in the compression zone. No cause of initiation found. Magnification setting on microscope = 20x

Figure 53 shows the second largest vented tree found with a length of 250 µm. The tree was inspected under the same conditions like the one in figure 52. However, in this sample, there is a slight unevenness in the inner semiconductor, which is likely the cause of initiation.

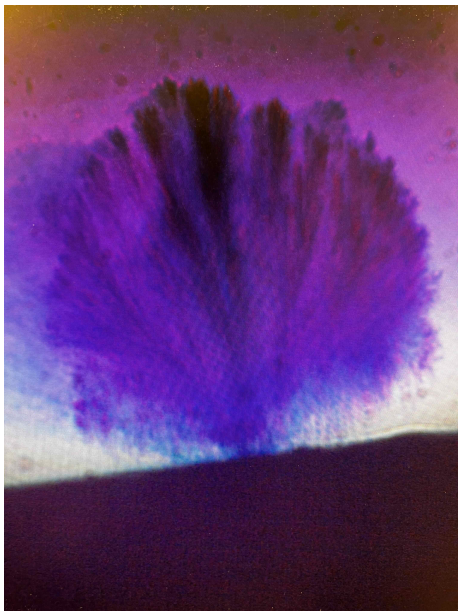

Figure 53: Picture of the second largest vented tree found. Length = 190 µm from the cable that was aged for five months. Located in the compression zone. Small unevenness is likely the reason for initiation. Magnification setting on microscope = 20x

5 Discussion

In this section the results, method, the impact of test conditions and sources of error will be discussed.

5.1 Bow-tie tree growth in XLPE with applied stretch and compression forces

5.1.1 Development of bow-tie tree length over time

The theory in subsection 2.2.3 explains that the growth pattern of a bow-tie, where the growth rate is generally quite steep initially, which rapidly settles down and saturates, as illustrated in figure 7. This growth pattern happens because of the high moisture available at the beginning and nearly halts as the onset moisture collects within hydrophilic regions. The hypothesis in subsection 1.4 assumes that the development of L_{max} of a bow-tie is dependent on several factor, one of which is aging time and that the mechanical force applied could alter the time needed before the growth of the bow-ties halt. The growth pattern of a bow-tie can be recognized in figure 40, 43 and 46. Confirming that the bow-ties somewhat stops growing after sufficient aging time. It is therefore not expected that the average maximum length will increase much more. Figure 49 with minimum compression force indicates a confirmation of the hypothesis that assumes the impact of mechanical forces applied alter the aging time needed before the growth rate halts. However, figure 46 with maximum compression contradicts the same hypothesis, as the growth pattern resembles the pattern seen in the maximum and minimum stretch. The trend of the β values of the bow-ties found in maximum stretch and compression shows that the condition of the cable gets worse over the time period of six months. There is a far higher chance of finding bow-ties with extreme lengths in the samples from the cables that have been aged for five and six month, showing that aging time is a big factor of water tree growth.

5.1.2 Water tree growth in cable loaded with stretch forces compared to compression forces

Another factor in the hypothesis that influences the length of water trees is the amount of stretch applied to the cable. Based on the theory, several forces acting on the insulation in the cable. Frozen in and Maxwell forces can work in the same direction to make voids and micro crazes in the insulation and semiconductor. The hypothesis in section 1.4 assumes that the static mechanical tension will work in conjunction with the frozen in and Maxwell forces and, therefore, enhance water tree growth while the compression force induced by bending the cable will diminish the growth.

According to research done by R. Patsch and A. Paximadakis initiation and growth of bow-tie trees is heavily dependent on stretch and compression forces on the in-

sulation. Where the longest and highest density of trees are found in the part of insulation that are under stretch forces [22][23]. Which is further confirmed by E. Ilstad and S. Nordås [4].

By comparing figure 40 and 46 the effect of stretch and compression can be seen more clearly. Where the L_{max} is longer in the stretch zone compared to the compression zone. However, the difference is small.

The same can be seen in the average maximum lengths η, which are also higher in the stretched zone than in the compression zone. The exception is in the three months of aging, where the two most extreme lengths of the bow-tie were longer in the compression zone than the stretched zone. However, the trend of the two figures confirms this hypothesis.

Another statement in the hypothesis was that the amount of stretch and compression would influence the results. The average maximum lengths η of the bow-ties in the maximum stretched cables and minimum stretched cables shows very little difference. An increase in 8% stretch only yields 7% increase in bow-tie length. This indicates that there are very little effect of the increased stretch forces (4% to 12%) on the average maximum length. However the extreme lengths increase slightly, imply that the stretch can enhance the growth of the largest bow-tie trees.

5.2 Vented tree growth in XLPE with applied stretch and compression forces

For a long time, it has been known that moisture in a medium and high voltage cable can cause water tree growth within the insulation and increase the probability of failure. Strand-fill, sometimes called moisture-block, is used as protection against moisture migration in the conductor. The gaps between each conductor strand are filled with a semi-conducting sealant during the stranding operation. The strand-fill does not cover the most outer strands and does not interfere with the conductor to conductor shield interface.

Figure 54: Picture of one of the test-objects cut open to confirm that there are strand-fill between gaps of the conductor strands

Due to the strand-fill in the cable objects, there was no longitudinal water migration, only radially in this experiment. The material composition of the insulation and inner- and outer semiconductor possibly have water tree retardant additives resulting in very little growth of water trees. The additives and strand-fill could also alter the conditioning time and, therefore, decrease the relative humidity inside the insulation. Resulting in the cable being conditioned with a lower relative humidity level than first planned and therefore with water tree growth at a reduced rate, as explained in subsection 2.2.5. These factors could play a role in the amount and length of the ventilated trees found

The locations of the vented water trees documented in the results section show no significant correlation between the amount or length of vented trees found in relation to stretch or compression forces. The amount of vented trees was also found to be highest in the zone with minimum stretch compared to maximum stretch.

None or a low amount of vented water trees in the outer semiconductor was expected. The results documented by E. Ildstad and S. Nordås shows that only 2% of the vented water trees were found at the outer semiconductor[19]. This is confirmed by the results in section 4.3, where only one vented tree was observed in the outer semiconductor.

One reason for the low amount of vented trees in the outer semiconductor can be explained by the frozen in forces. During the manufacturing process, the outer semiconductor is subjected to higher temperatures and more rapid cooling than the inner semiconductor. This can lead to significant differences in residual strains and crosslinking between XLPE and semiconductor[19].

Another factor that may be related is the difference in electric field strength. As shown in section 3.2, the field strength at the outer semiconductor will be $E_{min} \approx 4kV/mm$, which is 46% lower compared to the field strength at the inner semiconductor. As shown in theory section 2.2.2, the formula for the Maxwell forces is proportional to the electric field, and thus the reduction in field strength will reduce the Maxwell forces equally.

A third factor that can influence the initiation of vented water trees in the outer semiconductor is the material composition. Whereas the material composition of outer semiconductor often consists of nitrile rubber which enhances the flexibility. Therefore the stretch forces applied may have a smaller effect on the outer semiconductor than if the material composition were the same.

The longest vented trees observed was 250 µm and 190 µm. The largest vented tree was found in the minimum stretch zone with 5 months of aging. Based on the theory 2.2.3, the source or initiation point often comes from unevenness, abnormalities like trapped hydrophilic particles, or damage to the semiconductor[8]. However, largest tree seen in figure 52 there was no signs of damage to the semiconductor or unevenness and no visible trapped hydrophilic particle as seen in figure 55 below. The initiation point of the vented tree could be damage to the semiconductor or a craze going inwards which was not visible from above or below. This is why an attempt was made to tilt the microscope 45°to look towards the wall of the semiconductor. However, this attempt failed. As the focus point is narrow and the

sensitivity to the lighting control it was nearly impossible to get a clean focus.

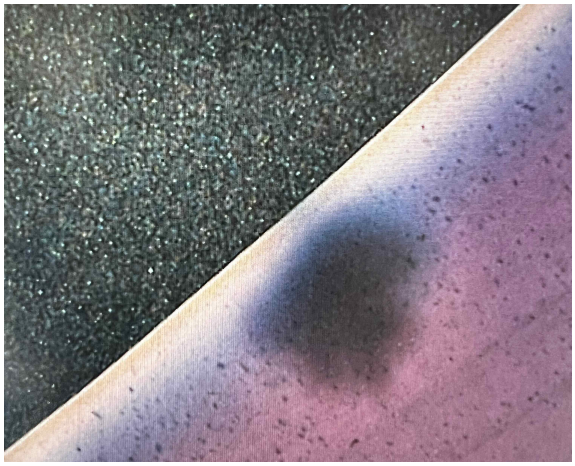

Figure 55: Picture of the inner semiconductor where the largest vented tree was found. Microscope magnification: 1000x

5.3 Sources of error

Some complications occurred during the process of applying static mechanical load to the cable 3.2.3. Due to the rigidity of the cable, the mechanical load on the screws to the cable clamps became too high, resulting in some screws being sheared off. These cable clamps secure the cable to the pipe and ensure that the cable follows the circumference of the pipe. This was fixed by using quick clamps on the failed connection points. The tension on these cables with the failed cable clamps may have been altered.

Furthermore, the pipe that represents the medium tension was made of wood. The wood cracked on some of the cable samples. Therefore, the tension altered, and in combination with the pipes not being completely submerged, resulted in consistently shorter bow-ties in this sample compared to the samples from the minimum stretch. In the third month of aging zero bow-ties was found from the medium stressed cable. It was, therefore, decided not to continue counting the samples from the medium stressed region as they were not reliable, and with to many factors that altered the results.

During the microscope analysis, several sources of error can occur. One of which is the calibration of the microscope used to measure the length of the water trees. To prevent this as far as possible the same microscope was used to do all the measurements to ensure as reliable measurements as possible. It was challenging to distinguish if a tree was within the zone of measurements or outside. If there was any doubt if the tree was within the zone or not, it was counted as within. Human error also needs to be taken into account. There is a possibility that water trees have been overlooked. The focus setting is crucial to see the different water trees when doing the microscope analysis. As it is adjusted, some trees disappear, and some appear. It can therefore be challenging to find the biggest tree.

6 Conclusion

In this thesis, six cables with applied static mechanical stress were examined. The mechanical stress was applied by bending the cables around pipes with different diameters resulting in $\epsilon = 12\%$ and $\epsilon = 4\%$ stretch. The test samples were placed in water at $40°C$ and energized with 30 kV AC 50 Hz. The first cable was aged for one month, whereas the other cable samples aged with time steps of one month, giving a total of six months of aging. During the microscope analysis, the length of the longest bow-ties in the stretch and compression zone was documented. Also the length of the ventilated trees and the zone it was observed in was documented.

It is documented that the static mechanical stresses influence the growth pattern of the bow-ties, where the average maximum length of the bow-ties is longer in the zone with stretch force applied than in the zone with compression force applied. The results also indicate that the most extreme lengths of the bow-ties are influenced by the stretch force applied, where the longest trees was mostly found in the samples with maximum stretch.

By comparing the maximum stretch and minimum stretch samples, the results imply that the average maximum length of the bow-ties increase with approximately the same amount, as the increase in stretch, where an 8% increase in stretch yields an average of 7% increased length. By comparing maximum compression with minimum compression, there is also an increase in maximum average length, with an increase of 8% compression force yields an increase of 10% in length.

The result shows that there is no significant difference in observed initiation of vented water trees when comparing the stretch zone with the compression zone. However, due to the limited amount of vented water trees observed, the results can only give an indication.

Even with high mechanical stress applied, and energized with voltage level of 2.5 times what it was designed for, the largest vented tree observed was $250\,\mu m$ which is 7% of the total insulation thickness.

7 Further work

Due to the material composition with the water tree retardant additives and strand-fill, this type of cable should be tested over a longer time period. It could therefore be interesting to continue testing on this setup with the 3 cables left connected to the test-rig. With the small increases in length of the water trees from month to month, the time steps between each cable should be extended, resulting in a total aging time of 1 year.

One factor that increases the water tree growth is aging with temperature gradient. If this testing method is going to be repeated, it is recommended to age with temperature gradient to accelerate the growth of vented water trees, which is needed to get more reliable results.

As the vented trees most often is the reason of breakdown in medium to high voltage cables, a closer inspection inside the root of the tree could be interesting. This however requires the use of electron microscope.

Bibliography

[1] Magnus Bøe. Future design of subsea high voltage cables for offshore renewables - effect of mechanical stresses on the insulation lifetime. Project report in TET5500, Department of Electric Power Engineering, NTNU – Norwegian University of Science and Technology, Dec. 2021.

[2] Kjeller Vindteknikk. *Vindkart for Norge*. NVE, 2009.

[3] Equinor. Hywind tampen: verdens første fornybare kraftkilde for olje- og gassvirksomhet til havs. https://www.equinor.com/no/what-we-do/hywind-tampen.html Accessed: 2021-12-02.

[4] E. Ildstad, S. Nordås, and T. A. Lindseth. Water treeing of xlpe cables under combined mechanical and electrical stress.

[5] F. Mauseth, M. Amundsen, and H. Faremo. Water tree growth of wet xlpe cables stressed with dc and high frequency ac voltage superimposed. In *Conference Record of IEEE International Symposium on Electrical Insulation*, pages 266–269, 2012.

[6] Truls Amundsen Lindseth. Vanntrevekst i mekanisk og elektriskpåkjente pex-kabler. Master's thesis, Norwegian University of Science and Technology, 2011.

[7] A Haddad, A Haddad, and D. F Warne. *Advances in High Voltage Engineering*, volume 40 of *IEE power and energy series v.40*. The Institution of Engineering and Technology, Stevenage, 2004.

[8] E.F. Steennis and F.H. Kreuger. Water treeing in polyethylene cables. *IEEE Transactions on Electrical Insulation*, 25(5):989–1028, 1990.

[9] J. Sletbak. The mechanical damage theory of water treeing-a status report. In *Proceedings of the 3rd International Conference on Properties and Applications of Dielectric Materials*, pages 208–213 vol.1, 1991.

[10] F. Mauseth, S. Hvidsten, H. Saeternes, and J. Aakervik. Influence of dc stress superimposed with high frequency ac on water tree growth in xlpe insulation, 2013.

[11] J. Henry. Next generation high voltage subsea transmission cables: Influence of electric field, nacl impurities and thermal cycling rate on insulation lifetime. Master's thesis, Norwegian University of Science and Technology, 2019.

[12] F. Mauseth. Tet4160 insulation materials for high voltage applications. NTNU Department of Electric Power Engineering, Trondheim.

[13] L.A Dissado. Electrical degradation and breakdown in polymers, 1992.

[14] Jordan Henry. Next generation high voltage subsea transmission cables: Influence of electric field, nacl impurities and thermal cycling rate on insulation lifetime., 2019.

[15] A. Abideen and F. Mauseth. Review of water treeing in polymeric insulated cables.

[16] S. HVIDSTEN S.M. Hellesø. Degradation rates in high voltage subsea cables with polymeric water barrier designs. *Jicable'15 - 9th International Conference on Power Insulated Cables : proceedings*, 2016.

[17] Simon Årdal Aarseth. Virkning av mekanisk spenning på vanntrevekst i pex isolerte høyspentkabler. Master's thesis, Norwegian University of Science and Technology, 2013.

[18] H. FAREMO S.M. HELLESØ, S. HVIDSTEN. Water tree ageing of high voltage xlpe cable insulation system under combined dynamic mechanical and ac eletrical stress. *CIGRE (Conseil international des grands réseaux électriques)*, 2014.

[19] Ståle Nordås and Erling Ildstad. The influence of strain on water treeing in xlpe power cables. In *2010 10th IEEE International Conference on Solid Dielectrics*, pages 1–4, 2010.

[20] Sintef. High voltage subsea cables: reducing costs by simplifying design. https://blog.sintef.com/sintefenergy/high-voltage-subsea-cables-reducing-costs-by-simplifying-design/ Accessed: 2021-12-06.

[21] S. Soady. Screen & semi-conductive layer on medium voltage cables. https://www.powerandcables.com/screen-semi-conductive-layer-on-mv-cables/ Accessed: 2021-12-06.

[22] A. Paximadakis and R. Patsch. The influence of mechanical stress on initiation and growth of bow-tie and boundary water trees, 1991.

[23] R. Patsch and A. Paximadakis. Water trees in cables-experimental findings and theoretical explanations. *IEEE Transactions on Power Delivery*, 5(2):767–773, 1990.

Appendix

A Bow-tie results from the microscope analysis

Table 10: Bow-tie results from the microscope analysis one to three months of aging

1 Month Bow-tie		
Sample:	**Min stretch**	**Min compression**
1	85.77	42.66
2	51.43	52.01
3	68.99	44.68
4	64.18	63.72
5	57.52	71.54
6	110.34	69.84
7	94.03	88.6
8	88.75	74.23
9	94.32	58.4
10	102.43	35.93

1 Month Bow-tie		
Sample:	**Max stretch**	**Max compression**
1	81.55	60.74
2	86.32	88.3
3	90.22	78.96
4	70.78	77.94
5	79.43	60
6	87.33	83.02
7	92.11	59.6
8	95.12	75.47
9	97.71	69.51
10	74.87	58.88

2 Month Bow-tie		
Sample:	**Min stretch**	**Min compression**
1	96.14	48.45
2	89.08	48.75
3	76.51	36.06
4	105.93	73.62
5	97.67	69.08
6	119.36	45.1
7	104.82	36.73
8	105.13	71.27
9	91.76	73
10	116.72	111.16

2 Month Bow-tie		
Sample:	**Max stretch**	**Max compression**
1	108.61	59.34
2	105.66	95.62
3	95.57	84.03
4	110.35	94.37
5	110.48	67.9
6	133.2	98.18
7	121.56	107.22
8	83.27	75.23
9	89.98	70.17
10	87.73	56.95

3 Month Bow-tie		
Sample:	**Min stretch**	**Min compression**
1	84.17	77.22
2	132.73	111.8
3	104.55	88.83
4	91.11	78.51
5	200.26	96.36
6	112.12	57.43
7	117.99	111.27
8	111.12	91.54
9	103.23	84.31
10	94.56	74.11

3 Month Bow-tie		
Sample:	**Max stretch**	**Max compression**
1	138.01	65.97
2	116.72	109.409
3	131.9	141.8
4	117.75	77.22
5	108.18	134.04
6	105.04	80.55
7	93.35	154.3
8	146.52	108.42
9	136.34	109.2
10	147.84	144.24

Table 11: Bow-tie results from the microscope analysis four to six months of aging

4 Month Bow-tie		
Sample:	**Min stretch**	**Min compression**
1	130.422	120.17
2	122.04	91.23
3	110.35	121.02
4	93.95	84.17
5	118.67	109.8
6	95.32	128.29
7	99.54	81.26
8	91.34	82.4
9	134.43	112.66
10	84.79	71.55

4 Month Bow-tie		
Sample:	**Max stretch**	**Max compression**
1	95.96	116.65
2	180.67	100.03
3	113.66	85.98
4	125.62	94.755
5	123.96	69.88
6	101.6	118.83
7	104.35	85.42
8	104.15	119.36
9	148.23	94.07
10	105.54	109.06

5 Month Bow-tie		
Sample:	**Min stretch**	**Min compression**
1	115.27	128.16
2	105.94	97
3	109.27	155.42
4	110.37	93.5
5	161.17	128.16
6	107.27	85.23
7	127.44	136.96
8	130.24	126.99
9	93.88	89.21
10	131.13	128.505

5 Month Bow-tie		
Sample:	**Max stretch**	**Max compression**
1	174.23	72.16
2	96.672	81.83
3	130.42	88.91
4	110.35	88.34
5	84.55	81.15
6	147.52	74.36
7	114.38	170.35
8	151.3	103.89
9	120.08	99.75
10	115.45	72.59

6 Month Bow-tie		
Sample:	**Min stretch**	**Min compression**
1	97.79	89.67
2	94.2	82.75
3	93.63	96.23
4	131.68	86.42
5	129.16	97.37
6	102.53	73.41
7	95.22	82.75
8	103.54	100.11
9	93.1	93.56
10	104.66	100.49

6 Month Bow-tie		
Sample:	**Max stretch**	**Max compression**
1	131.91	71.55
2	94.04	203.63
3	90.32	101.62
4	97.74	175.72
5	127.91	106.45
6	142.56	60
7	109.16	101.81
8	127.62	116.54
9	103.55	85.06
10	96.13	86.3

B Vented water tree results from the microscope analysis

Table 12: Vented tree results from the microscope analysis after 6 months of aging

Month	Stretch [µm]	Compression [µm]
1 Month	0	0
2 Month	54.6 89.03 70.17	59.70 51.42 103.17 41.03
3 Month	73.54	59.33 46.24
4 Month	37.53 29.61 66.29 31.00	32.13 45.67 59.33 87.32
5 Month	81.04 165.44 84.02	250.1 52.97 190.45 51.31 74.23 48.31
6 Month	99.45 35.53	0

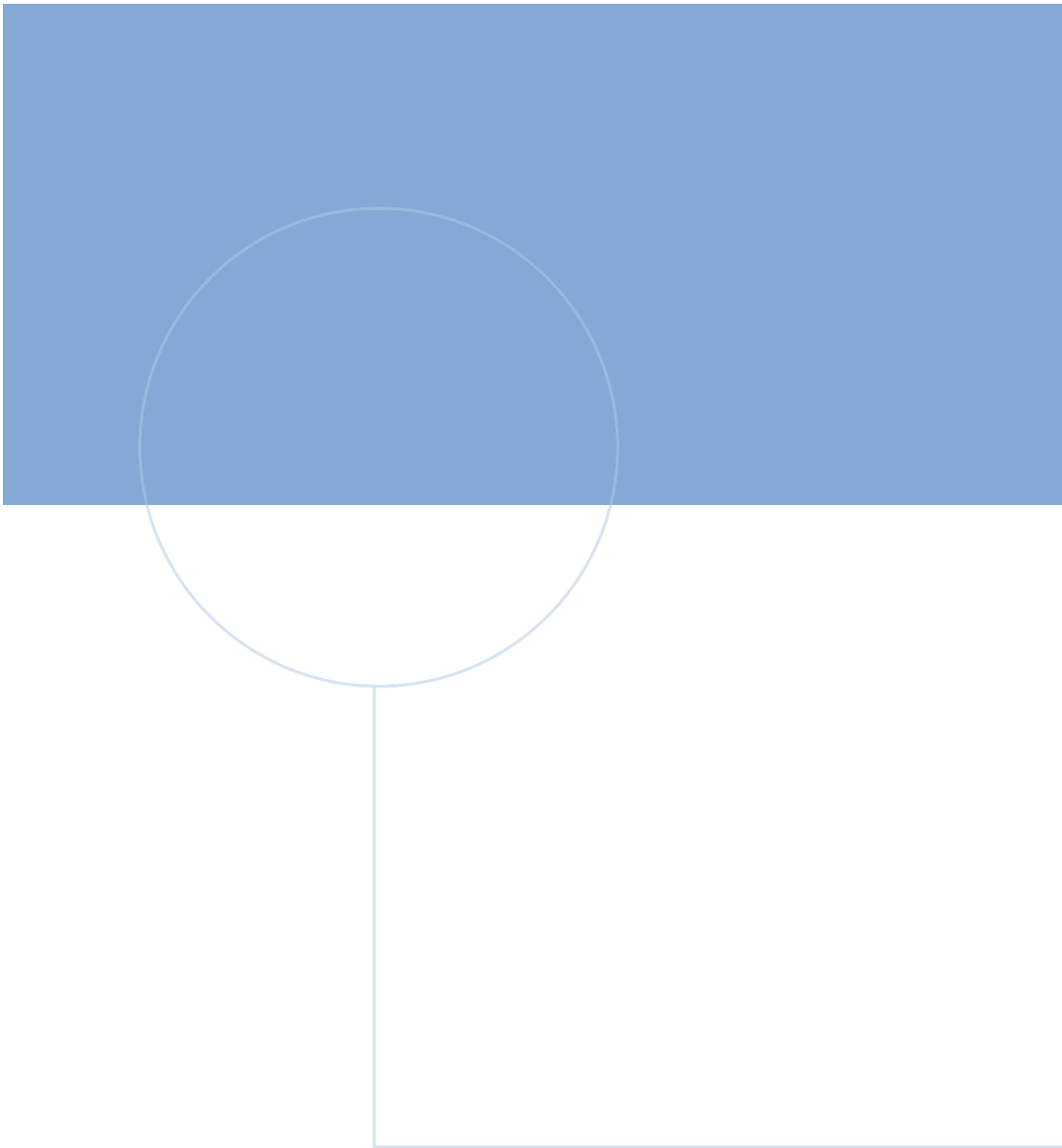

NTNU

Kunnskap for en bedre verden